高知工科大学
KOCHI UNIVERSITY OF TECHNOLOGY

Study on the dynamics of golf swing and impedance control for a golf swing robot

著者	Chen Chaochao
year	2007-03
学位授与番号	26402甲第111号
URL	http://hdl.handle.net/10173/361

Study on the dynamics of golf swing and impedance control for a golf swing robot

Chaochao Chen

A dissertation submitted to
Kochi University of Technology
in partial fulfillment of the requirements
for the degree of

Doctor of Philosophy

Graduate School of Engineering
Kochi University of Technology
Kochi, Japan

February 2007

Abstract

Jorgensen [1] said that “Golf, with its intense frustrations, bitter disappointments, sturdy enjoyments, and, yes, extreme ecstasies, would not be the game it is without the continual dream to do better the next time around.” In golf, every shot demands the satisfaction of two requirements: (1) distance; and (2) accuracy. The maximum distance off the tee with a driver club is certainly what all golfers strive for. In order to hit a drive of maximum distance, the club head must be traveling at maximum speed at impact of club and ball [2]. A golfer wishing to achieve this goal may find himself overwhelmed by books, magazines, and other golfers. However, it is no doubt that the wrist action for a golfer during the golf swing is a considerably important factor in the determination of the final club head speed [1-2]. To investigate the roles of different patterns of wrist actions (negative, positive, and negative-positive torque at the wrist) during the golf downswing, two optimization methods (maximum and impact criteria) are separately used in a two-dimensional double pendulum model of golf downswing to determine what extent wrist action increases club head speed in a driver, and affects optimum ball position. On the other hand, to more appropriately emulate the downward phase of golf swing, a new two-dimensional and two-segment model of golf downswing, in which the bending flexibility and centrifugal stiffening of golf shaft are taken into account, is utilized to examine whether the combination of ball position and wrist action (various patterns of torque applications) can increase club head speed at impact.

In recent years, golf swing robots have been used instead of professional golfers for the evaluation of golf club performance because the evaluation process for the development of new golf clubs by professional golfers occupies considerable time and

resources. Golf swing robots currently on the market usually have two or three joints, which are connected by gears and belts with completely interrelated motion. In addition, the joints are always controlled during the swing by the specified club head speed. Various golfers, however, show different swing styles even if they hold the same golf club. This phenomenon casts light on the significance of the interaction between a golfer's arms and a golf club. In order to gain a clear understanding of how the interaction influences the golf swing, a two-dimensional double pendulum model of the golf swing is employed and simple theoretical equations using normalized parameters are derived. The results, from the normalized-parameter equations, show that the length and, in particular mass ratios of clubs to arms are important parameters which eventually affect impact time, horizontal club head speed and club positions at impact. Unfortunately, although the dynamic interaction will result in different swing motions even if the robot has the same input torque of the shoulder joint as that of a golfer, the influence of the dynamic interaction has not been considered in the conventional control of a golf swing robot An impedance control method is thus proposed for a golf swing robot to emulate different-arm-mass golfers in consideration of the dynamic interaction between a golfer's arms and a golf club. In order to simulate the swing motions of different-arm-mass golfers, a new two-dimensional and two-segment model of golf downswing is established. The impedance control method is implemented to a prototype of golf swing robot comprising one actuated joint and one passive joint. The comparison of the swing motions between the robot and different-arm-mass golfers is made and the results show that the proposed golf swing robot with the impedance control method can emulate the swing motions of different-arm-mass golfers.

Contents

Chapter 1

Introduction

1.1 Research Background

The dynamics of golf swing have been studied for many years in an effort to improve the swing skills of golf players and to optimize the design of a golf club [1-12, 34-39]. The golf swing has been always modelled as a planar two linked system, named the "double pendulum" with the upper fixed pivot located at a point between the left shoulder and chest and the lower pivot point at the player's wrist joint [1- 7]. Most of these studies have regarded the golfer's arms and golf club as rigid rods [1-5], but others modelled the golf shaft as a flexible link [6-7]. Several researchers have presented a three-segment planar model that incorporated truck rotation (about the spine) in addition to the shoulder and wrist actions [8-10]. Note that the validity of the two-link model (arm and club), in particular for the rigid-rod system, has been confirmed by many researchers through actual swing experiments. That is, the known inputs for the model (input torques of shoulder and wrist) would result in the outcome, including the club head speed and the arm/club positions during the downswing, which is very much the same as that from actual golfers' swings. For example, Jorgensen [3] used the assumed constant shoulder torque to drive the model, and found that the club head speed was consistent with that from a professional's swing; Williams [5] applied the input torques of shoulder and wrist, obtained from the pictures of Bobby Jones's swing using inverse dynamics, to the model, and found that the swing motions of the arm and club in simulation agreed with those

from pictures. Such work was, however, lacked in the field of golf swing modelling where the flexible golf shaft or three-segment bodies is included.

The wrist action of a golfer is deemed to be of great significance in the determination of his final club head speed. To date, researchers have been asking: what kind of wrist action can provide an advantage in club head speed. In order to find the answer, a large number of dynamic models of golf downswing have been developed [1-10]. Using a two-rigid-segment and two-dimensional linked system, Williams [5] stated that neutral (zero) wrist torque was employed by the legendary golfer, Bobby Jones, at the latter stage of the downswing. Considering the bending flexibility of golf shaft, Suzuki & Inooka [6] also thought that the neutral wrist torque should be used in order to effectively utilize the shaft elasticity. But Jorgensen [3] and Cochran & Stobbs [2] found that the negative wrist torque (the so-called "late hit") could increase the club head speed, using the same model as that in Williams [5]. Milne & Davis [7], using a two-segment and two-dimensional model in consideration of shaft bending, suggested that a negative wrist torque before impact decreased the club head speed. This finding was consistent with the point of Budney & Bellow [4]. Jorgensen [3] and Cochran & Stobbs [2] stated that the club head speed could be improved by the appropriately "timed" positive wrist torque. Based on a three-rigid-segment model, Sprigings & Neal [10] also confirmed the role of the positive wrist torque in the improvement of the club head speed.

All the golf ball positions at which impact occurs were, however, constant in their work. Since the ball position played an important role in the improvement of the final club head speed [11], the ball position in this paper is not assumed to be constant but a variable in the optimization models.

To date, many types of golf swing robots have been developed. For these robots, the swing motions of various professional golfers were expected to be emulated by them and the evaluation of the golf club performance by humans to be replaced.

Although much progress has been achieved in this area, there still remains a long-standing challenge for a golf swing robot to accurately emulate the fast swing motions of professional golfers. It has been noticed that conventional golf swing robots on the market are usually controlled by the swing trajectory functions of joints or of the club head directly measured from professional golfers' swings. The swing motions of these robots, unfortunately, are not completely the same as those of the advanced golfers, in that they do not involve the dynamic interactions featured by different characteristics of golfers' arms and golf clubs. Suzuki & Inooka [12] proposed a new golf swing robot model consisting of one actuated joint and one passive joint. In their model, the robot like professional golfers, was able to utilize the interference forces resulting from the dynamic features of individual golf clubs on the arms, and the corresponding optimal control torques of the shoulder joint could be obtained. Ming & Kajitani [13] gave a new motion planning method for this type of robot to gain the optimal control torques by using different cost functions. The control input for the robot in their work was the torque function of the shoulder joint instead of the general ones such as the trajectory functions of joints or of club head. The change of the control input mainly results from the special dynamical characteristics of this new type of robot: the swing motion of the wrist joint is generated by the dynamic coupling drive of the shoulder joint. This point was specifically explained in the work of Ming & Kajitani [13]. In their research, however, the difference between the golfer's arm and the robot's arm in mass (or the moment of inertia of arm)

was not considered. In order to indicate the vital of a golfer's arm mass, a two-dimensional double pendulum model of golf swing with normalized parameters is established. The simulation results clearly show that the mass ratio of clubs to arms and the arm mass are important factors to influence the golf swing performance. Therefore, if the optimal control torque from their work [12-13] is applied to other golfers who own different-mass arms, the various swing motions would occur. In other words, the robots proposed by them at most can emulate one kind of golfers who must have the same arm mass as that of the robot. The limitation of the golf swing robots promotes us to investigate a new control method to make the robots emulate more general golfers.

1.2 Research Objectives

The objectives of this dissertation are first to investigate what kind of wrist action can improve the horizontal club head speed at impact in consideration of the golf ball position, and to determine the optimum ball position at impact for various types of wrist actions; and second, to make a prototype of golf swing robot emulate swing motions of different-arm-mass professional golfers, using an impedance control method.

The dissertation is organized as follows: Chapter 2 gives the wrist action study using a two-dimensional double pendulum model of golf downswing. A new two-dimensional model of golf downswing considering the bending flexibility and centrifugal stiffening of the golf shaft is established to investigate the role of the wrist action in chapter 3. Chapter 4 is devoted to the understanding of the importance of the dynamic interactions between humans' arms and golf clubs during the golf swing. An impedance control method for a prototype of golf swing robot is developed in Chapter 5. Conclusions are drawn in Chapter 6.

Chapter 2

Study on the wrist action in a double-pendulum swing model

2.1 Mathematical model

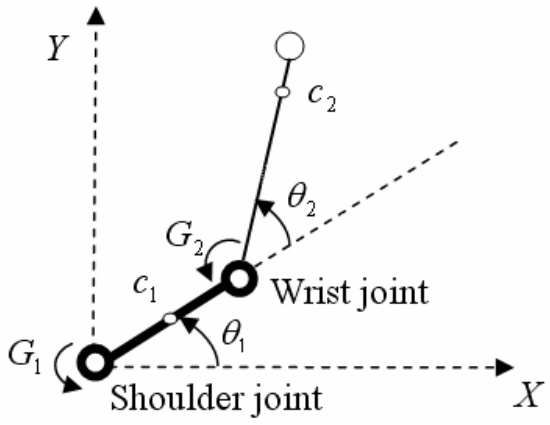

Figure 2-1 Double pendulum model of golf downswing. c_1, c_2 are the centers of the mass of arm and club, respectively. The X axis is parallel to the target line on the ground

As shown in Figure 2-1, the mathematical model of golf downswing is deemed to a 2-dimensional double pendulum. This model consists of a rigid arm link and a rigid club link. It is assumed that the swing takes place in a plane tilted ϕ to the ground. The assumption of the planar movement of the downswing is well supported in the work of Cochran & Stobbs [2] and Jorgensen [1].

The downswing is separated into two phases: phase 1 and phase 2. In phase 1, the two rigid bodies rotate as one body with a constant wrist-cock angle. In phase 2, the various types of wrist actions are employed.

The following notation is applied:

G_1, G_2	Torque on arm and club, respectively
m_1, m_2	Mass of arm and club, respectively
a_1, a_2	Length of arm and club, respectively
l_1, l_2	Length from shoulder joint to c_1 and from wrist joint to c_2, respectively
I	Moment of inertia of arm about shoulder joint
J	Moment of inertia of club about c_2
θ_1, θ_2	Angle of arm and club, respectively
ϕ	Inclination of plane of downswing
g	Acceleration of gravity

Table 2-1. Parameter values of swing model

m_1	7.312 kg
a_1	0.615 m
l_1	0.326 m
I	1.150 kg. m^2
m_2	0.394 kg
a_2	1.105 m
l_2	0.753 m
J	0.077 kg. m^2
ϕ	60°

The parameter values of the arm and club applied in the calculation are those given by Lampsa [14]. All the parameter data is shown in Table 2-1 and the club data is considered to be appropriate for a driver. The equations of motion of the model are derived from the Lagrangian method. The detailed equations in two phases are given as follows.

In phase 1:

$$\begin{aligned}&\left(I+J+m_2 l_2^2+m_2 a_1^2+2m_2 l_2 a_1 Cos\theta_2\right)\ddot{\theta}_1+\left(J+m_2 l_2^2+m_2 l_2 a_1 Cos\theta_2\right)\ddot{\theta}_2\\&-\left(2\dot{\theta}_1+\dot{\theta}_2\right)m_2 l_2 a_1 Sin\theta_2\,\dot{\theta}_2\\&+g\,Sin\phi\left(m_2 l_2 Cos\left(\vartheta_1+\theta_2\right)+\left(m_1 l_1+m_2 a_1\right)Cos\theta_1\right)=G_1\end{aligned} \tag{2-1}$$

$$\left(J+m_2 l_2^2\right)\ddot{\theta}_2=0 \tag{2-2}$$

In phase 2:

$$\begin{aligned}&\left(I+J+m_2 l_2^2+m_2 a_1^2+2m_2 l_2 a_1 Cos\theta_2\right)\ddot{\theta}_1+\left(J+m_2 l_2^2+m_2 l_2 a_1 Cos\theta_2\right)\ddot{\theta}_2\\&-\left(2\dot{\theta}_1+\dot{\theta}_2\right)m_2 l_2 a_1 Sin\theta_2\,\dot{\theta}_2\\&+g\,Sin\phi\left(m_2 l_2 Cos\left(\vartheta_1+\theta_2\right)+\left(m_1 l_1+m_2 a_1\right)Cos\theta_1\right)=G_1\end{aligned} \tag{2-3}$$

$$\begin{aligned}&\left(J+m_2 l_2^2+m_2 l_2 a_1 Cos\theta_2\right)\ddot{\theta}_1+\left(J+m_2 l_2^2\right)\ddot{\theta}_2\\&+m_2 l_2 a_1 Sin\theta_2\,\dot{\theta}_1^2+g\,Sin\phi\,m_2 l_2 Cos\left(\vartheta_1+\theta_2\right)=G_2\end{aligned} \tag{2-4}$$

2.2 Optimization method

Two optimization methods are used in our simulation: one is the maximum criterion, and the other is the impact criterion. The maximum criterion is used to achieve the maximum horizontal club head speed at impact; and the impact criterion is utilized to obtain the optimal golf club position at impact.

2.2.1 Maximum criterion

First, the criterion of maximal horizontal club head speed at impact (maximum criterion) is used to investigate the effects of different kinds of wrist actions on the golf downswing. The following equation indicates the maximum criterion.

$$-a_1\left(Sin\theta_1\,\ddot{\theta}_1+Cos\theta_1\,\dot{\theta}_1^2\right)-a_2\left(Sin(\theta_1+\theta_2)(\ddot{\theta}_1+\ddot{\theta}_2)+Cos(\theta_1+\theta_2)(\dot{\theta}_1+\dot{\theta}_2)^2\right)=0 \quad (2\text{-}5)$$

Eq. 2-5 is obtained by differentiating the equation of the horizontal club head speed v_h.

$$v_h=-a_1\,Sin\theta_1\,\dot{\theta}_1-a_2\,Sin(\theta_1+\theta_2)(\dot{\theta}_1+\dot{\theta}_2) \quad (2\text{-}6)$$

with respect to time, and then making it equal to zero..

The function of **NDSolve** in MATHEMATICA 5.2 is used to drive the simulation model. To obtain the swing motions of arm and club at impact including $\theta_1(t_{imp}),\theta_2(t_{imp}),\dot{\theta}_1(t_{imp}),\dot{\theta}_2(t_{imp})$ by the maximum criterion, the root of Eq. 2-5, impact time t_{imp}, is solved by the function of **FindRoot** that makes the left-hand side of Eq.2-5 less than 10^{-6} in magnitude. The impact time t_{imp} is then applied in the function of **NDSolve** to achieve angles and angular velocities of the arm and club at impact.

After obtaining the swing motions of the arm and club at impact, the maximal horizontal club head speed v_m is achieved, as shown in Eq.2-7.

$$v_m=-a_1\,Sin(\theta_1(t_{imp}))\dot{\theta}_1(t_{imp})-a_2\,Sin(\theta_1(t_{imp})+\theta_2(t_{imp}))(\dot{\theta}_1(t_{imp})+\dot{\theta}_2(t_{imp})) \quad (2\text{-}7)$$

The optimum ball position dx at impact is given by

$$dx=a_1\,Cos(\theta_1(t_{imp}))+a_2\,Cos(\theta_1(t_{imp})+\theta_2(t_{imp})) \quad (2\text{-}8)$$

2.2.2 Impact criterion

It has been reported by McLean [15] that the shaft positions of many professional

golfers are always maintained vertical at impact when viewed 'face-on', the impact criterion (vertical club shaft at impact) is thus applied to examine the role of the wrist action.

The impact criterion is given by.

$$\theta_1(t_{imp}) + \theta_2(t_{imp}) - 270^\circ = 0. \tag{2-9}$$

The function of **FindRoot** is used to obtain the impact time t_{imp} via making the left-hand side of Eq.2-9 less than 10^{-6} in magnitude. Then the club head speed and ball position at impact are achieved just using the same method as that in the maximum criterion.

2.3 Wrist action simulation

Three patterns of wrist actions including passive, active and passive-active are studied by the maximum and impact criteria. Six positive constant wrist torques are employed (5 Nm, 10 Nm, 15 Nm, 20 Nm, 25Nm and 30 Nm). Here, the maximal wrist torque (30 Nm) is given by Neal et al. [16], who measured this upper value of wrist torque from a low handicap amateur using inverse dynamics.

For the passive wrist action (PW), the arm release angle θ_1^r (given by Eq.2-10), that denotes when the wrist joint can be turned open, is delayed in every degree from the 'natural release point' until the point at which the regulated negative wrist torque is reached (the absolute value of the regulated negative wrist torque is the same as that of the positive wrist torque but with an opposite sign. For example, the regulated negative wrist torque is -30 Nm, if the positive wrist torque is 30 Nm).

$$\theta_1^r = \theta + p1, p1 = 1^\circ, 2^\circ \cdots, \theta_1^p \tag{2-10}$$

Where θ is the integer part of θ_1^n; θ_1^n, in this chapter, is the arm rotational angle when the 'natural release point' is reached; θ_1^p is the arm rotational angle when the regulated negative wrist torque is reached.

For the active wrist action (AW), the onset and termination of the positive wrist torque are determined when the arm rotational angle satisfies Eq.2-11 and Eq.2-12, respectively.

$$\theta_1^o = \theta + p2,\ p2 = 1^\circ,\ 2^\circ \cdots, \theta_1^\circ\left(t_{imp}\right) - 1^\circ. \tag{2-11}$$

$$\theta_1^t = \theta_1^o + p3,\ p3 = 1^\circ, 2^\circ \cdots, \theta_1^\circ\left(t_{imp}\right) \tag{2-12}$$

where θ is the integer part of θ_1^n; θ_1^o and θ_1^t are the arm rotational angles when the positive wrist torque is activated and deactivated , respectively; $\theta_1^\circ\left(t_{imp}\right)$ is the arm rotational angle when impact occurs;

For the passive-active wrist action (PAW), the negative wrist torque is applied, and then followed by the positive wrist torque. The application of the negative wrist torque is the same as that in the PW, in which the negative torque keeps the wrist-cock angle constant until the desired arm release angle θ_1^r is reached. The onset and termination of the positive wrist torque, following the passive wrist action, are given by Eq.2-13 and 2-14, respectively

$$\theta_1^{o1} = \theta_1^r + p4,\ p4 = 0^\circ, 1^\circ, \cdots, \theta_1^\circ\left(t_{imp}\right) - 1^\circ. \tag{2-13}$$

$$\theta_1^{t1} = \theta_1^\circ\left(t_{imp}\right). \tag{2-14}$$

Where θ_1^{o1} and θ_1^{t1} are the arm rotational angles as the positive wrist torque is activated and deactivated, respectively; $\theta_1^\circ\left(t_{imp}\right)$ is the arm rotational angle when impact occurs;

The natural release wrist action (NW), where no wrist torque is employed after the 'natural release point', is also studied for the purpose of comparison with the three wrist actions as mentioned above.

We assume that the simulation process commences when the golfer had just completed his backswing and was about to begin his downswing. Lampsa [14] thought that a pause usually occurred at this moment, indicating that the angular velocities of arm and club are zero. Thus we chose the following initial conditions for the downswing.

$$\theta_1(0) = 90^\circ, \dot{\theta}_1(0) = 0; \theta_2(0) = -90^\circ, \dot{\theta}_2(0) = 0. \tag{2-15}$$

It has been noted that there are many types of torque functions of shoulder joint applied in the previous research. Jorgensen [1] and Pickering & Vickers [11] considered that the shoulder input torque was constant during the downswing; Milne & Davis [7] used a ramp as the torque function and Suzuki & Inooka [6] set the torque function as a trapezoid. In the present study, the input torque of shoulder joint G_1 is assumed to be constant during the downswing as that in Jorgensen [1] and Pickering & Vickers [11]. The value of G_1 is chosen as 110 Nm which make the swing like that of a professional golfer (the horizontal club head speed at impact can reach 47.0741 m/s using NW).

2.4 Energy analysis method

As far as the authors are aware, the way the wrist action alters the club head speed at impact has not been given thoroughly, although some researchers did involve this point in their work. Jorgensen [3] attributed the role of the passive wrist action to the change of a mysterious term 'timing', yet the explicit explanation was not presented. Sprigings & Mackenzie [9] used a three-segment model comprising torso, arm and golf club to

identify the mechanical sources of power that are responsible for the increase in club head speed. The ball position, however, remained constant in their simulation model, and thus the influence of ball position upon the energy transference between the arm and golf club at impact was neglected. In the current study, we show how the wrist action affects the club head speed from an energy based analysis, when the ball position is not constant but determined by two criteria.

The work and power generated by a golfer are given by

$$E = \int P_1 \, dt + \int P_2 \, dt \tag{2-16}$$

$$P_1 = \tau_1 \, \dot{\alpha} \tag{2-17}$$

$$P_2 = \tau_2 \, \dot{\beta} \tag{2-18}$$

where E is the total woke produced by a golfer; P_1 and P_2 are the power generated from the shoulder and wrist joints, respectively.

The efficiency index of swing motion, η, is introduced, which is expressed as

$$\eta = \frac{K_4}{E} \tag{2-19}$$

Where K_4 is the horizontal component of the kinetic energy associated with the club head.

2.5 Results and discussion

Figure 2-2 shows the maximal horizontal club head speed at impact using three patterns of wrist actions (PW, AW and PAW), plotted against the wrist torque by the maximum criterion. The figure clearly shows that the larger wrist torque gives a better improvement in the horizontal club head speed at impact. We also note that the increase in speed can be gained for all kinds of wrist actions, as compared to NW. It is fairly clear

that PAW results in a higher club head speed at impact when compared to PW and AW with the same wrist torque. For example, when wrist torque is 15 Nm, PAW gives the highest horizontal club head speed at impact, 50.3454 m/s, which is 6.9 % greater than that of NW; while PW and AW result in the increases by 1.4 % and 5.6 %, respectively.

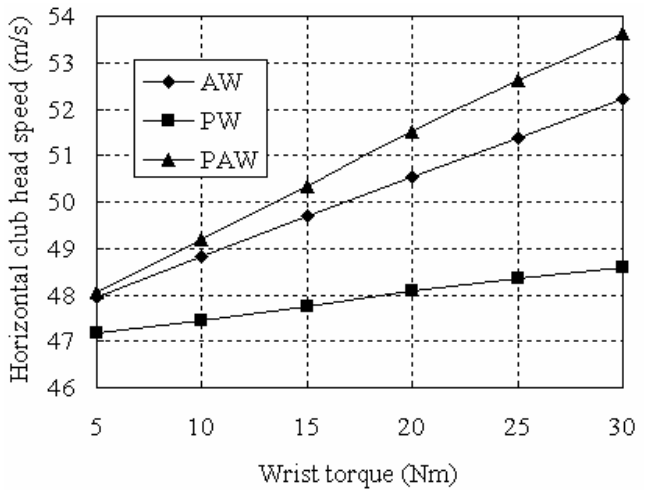

Figure 2-2 Maximal horizontal club head speed at impact by maximum criterion.

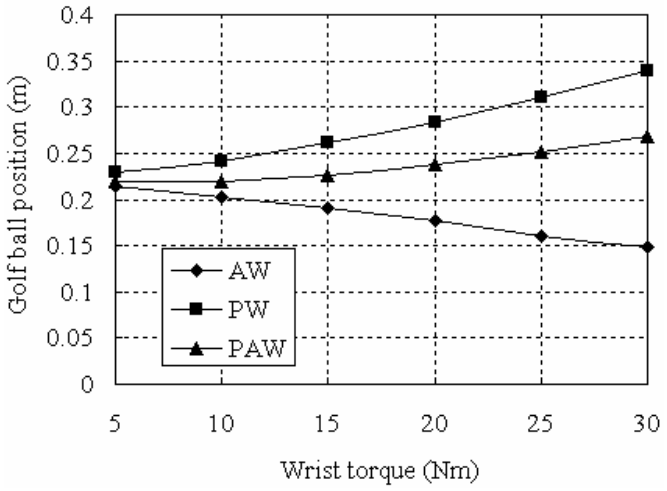

Figure 2-3 Optimum golf ball position by maximum criterion.

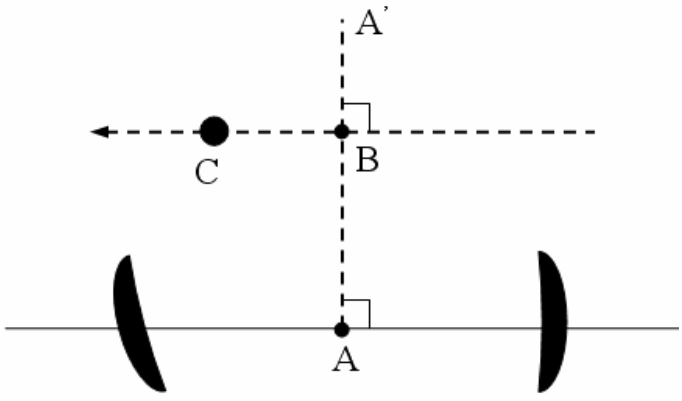

Figure 2-4 Golf ball position for a right-handed golfer when viewed overhead. Point C is the ball position and line AA' goes through the center of stance.

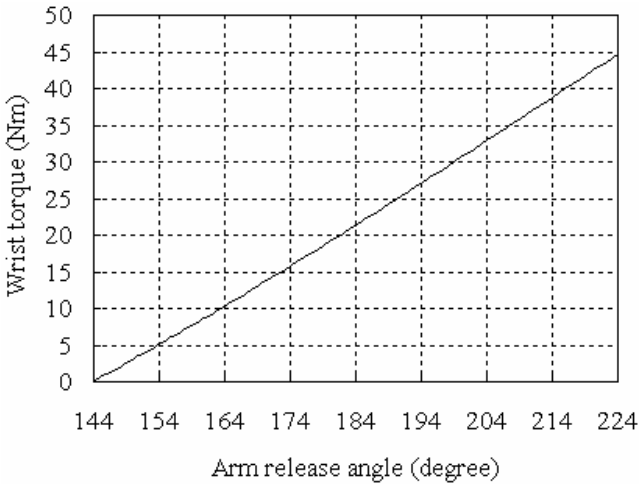

Figure 2-5 Required wrist torque when the arm release is delayed (the so-called 'late hit')

The optimum golf ball position at impact by the maximum criterion is shown in Figure 2-3. The ball position is defined for a right-handed golfer with the horizontal displacement BC, as shown in Figure 2-4. As we can see from Figure 2-3, the optimum ball position is determined by the various types of wrist actions and wrist torques. Figures 2-2 and 2-3 show that for PW, the increase in the horizontal club head speed is achieved when the ball is far away from the center of the golfer's stance (large ball position). This result is consistent with the conclusion of Pickering & Vickers [11]. It is known that the

large ball position needs a relatively large arm release angle (the so-called ‘late hit’) to achieve maximal club head speed when the passive wrist action is used (Pickering & Vickers [11]). Figure 2-5 shows that a large arm release angle requires such a high wrist torque that even exceeds the limit of 30 Nm (Neal et al, [16]). It thus appears to be an impracticable situation for golfers using passive wrist action to obtain the improvement of horizontal club head speed when the ball position is too large, since humans can never provide such a huge wrist torque to achieve the desired arm release angle. For PAW, Figures 2-2 and 2-3 show that the large ball position also gives the increased horizontal club head speed. However, it should be noted that the optimum ball position is obviously smaller than that for passive wrist action. Figures 2-2 and 2-3 also show that the relatively small ball position is able to provide an improvement of horizontal club head speed for AW.

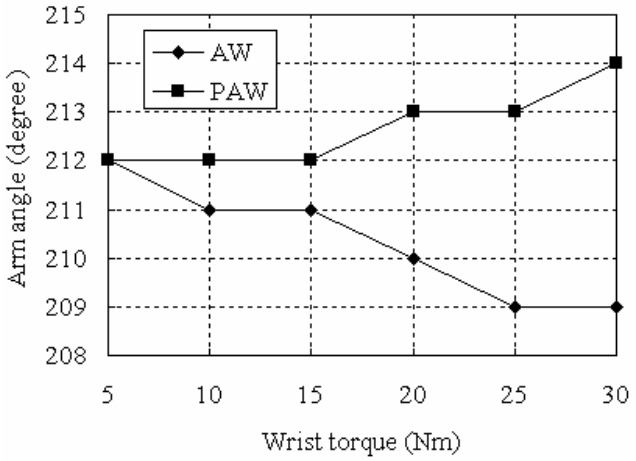

Figure 2-6 Arm angle when the optimum activation of positive wrist torque occurs

For AW and PAW, the arm rotational angle is used to describe when the optimum timing for the activation of positive wrist torque occurs (Figure 2-6). As we can see, the optimum timing for the activation occurs when the arm link approximately reaches the

angle of 210°. This result agrees well with that from Jorgensen [1] and Sprigings & Neal [10]. We also observe that the optimum activation changes slightly with the wrist torque.

As is reported by Cochran & Stobbs [2], the timing for the activation of positive wrist torque was able to influence the club head speed at impact. We examined this point in our simulation by advancing and delaying the optimum activation of positive wrist torque (Figure 2-7). For AW, if the activation of positive wrist torque is advanced as the arm angle arrived at 180°, the horizontal club head speed at impact is reduced by 0.8 %; when the activation is delayed until the arm angle reaches 230°, the reduction is 0.3 %. For PAW, the decreases are 0.8 % and 0.2 %, respectively.

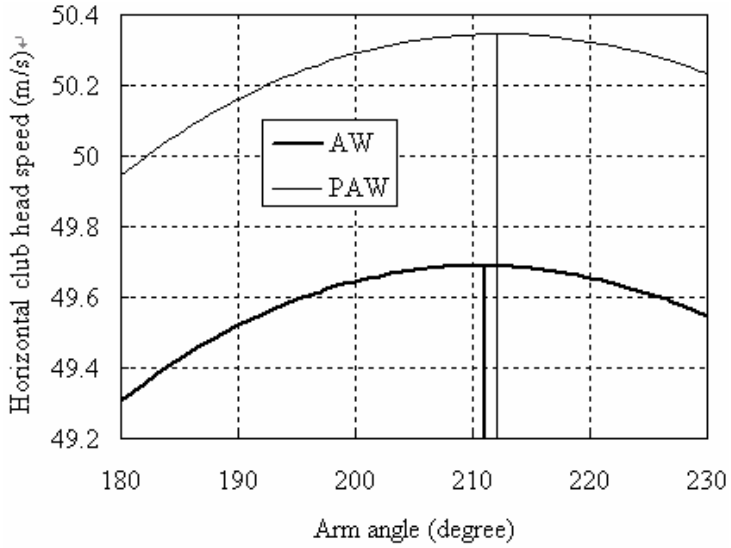

Figure 2-7 Horizontal club head speed at impact with different 'timed' activation of positive wrist torque (15 Nm). The thick vertical line shows the optimum activation for AW; the thin vertical line indicates the optimum activation for PAW;

The simulation results also show that the horizontal club head speeds at impact by maximum and impact criteria are almost the same for NW and PW. The maximal speed difference between them is merely 0.0002 m/s for NW and 0.0008 m/s for PW. The optimum ball positions are also almost equal between them. The maximal difference of

ball position is 4 mm and 8 mm for NW and PW, respectively. On the basis of these results, it can be concluded that for the golfers whose wrist actions belonging to NW or PW, the simple way to determine the optimum ball position is to put the ball at the position where the shaft is vertical at impact when viewed 'face-on'. This theoretical finding is consistent with the actual shaft position at impact that was observed from the numerous swing photographs of professional golfers such as Hogan, Lietzke, Nicklaus, Norman, Nelson, Peete, Price, Snead, Woods (McLean [15]).

For AW and PAW, the maximal difference in speed between the two criteria is 0.0797 m/s and 0.0785 m/s, respectively; and the maximal difference of ball position is 78mm and 73 mm, respectively. The optimum ball position at impact by the two criteria is shown in Figure 2-8. We note that the ball position by the maximum criterion is larger than that by the impact criterion, and the position difference becomes larger with the increase of the wrist torque. However, due to the small difference in the horizontal club head speed at impact by the two criteria (the maximal difference is only 0.0797 m/s), the impact criterion can be regarded as a reliable reference to obtain the optimum ball position for AW and PAW.

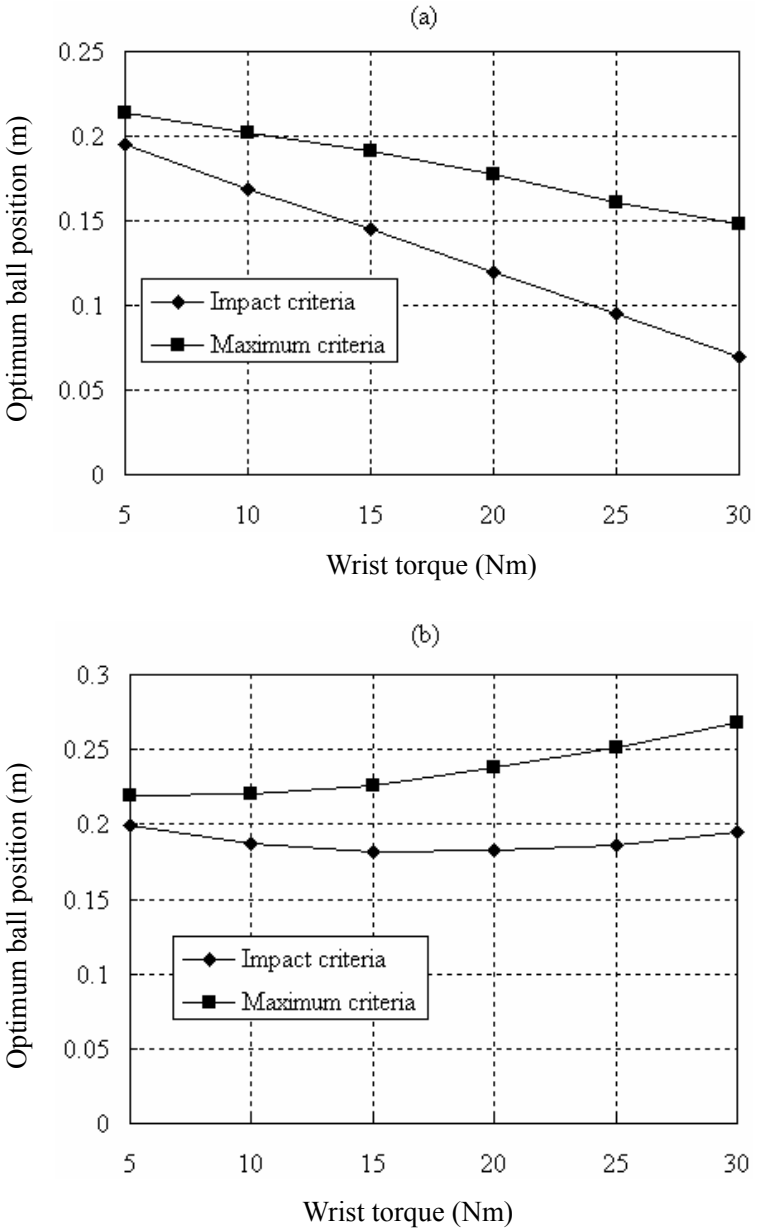

Figure 2-8 Optimum ball position by impact and maximum criteria (a) AW; (b) PAW

Table 2-2. Work and kinetic energy at impact (J)

Work and energy	NW		PW with 15 Nm		AW with 15Nm		PAW with 15Nm	
Total work	431.5	%total	438.4	%total	437.7	%total	444.0	%total
Work by shoulder joint	386.0	(89.5)	392.9	(89.6)	373.2	(85.3)	379.9	(85.6)
Work by wrist joint	0	(0)	0	(0)	18.2	(4.2)	18.2	(4.1)
Work by gravity	45.5	(10.5)	45.5	(10.4)	46.3	(10.5)	45.9	(10.3)
Kinetic energy of arm	142.7	(33.1)	140.8	(32.1)	118.7	(27.1)	116.5	(26.2)
Kinetic energy of club head	227.3	(52.7)	234.3	(53.4)	253.2	(57.8)	260.3	(58.6)

A set of comparisons in work and kinetic energy are undertaken among NW, PW, AW and PAW, and here, we use 15 Nm wrist torque. It should be noted that other wrist torques show different comparison results, but the overall way the wrist action affects the club head speed is not altered in nature. Table 2-2 shows the work and kinetic energy of arm and club head at impact by the maximum criterion. It can be seen that all the total work for PW, AW and PAW are increased as compared to that for NW. For PW, the higher total work obviously results from the increase of work produced by shoulder joint, because the negative wrist torque maintains the wrist-cock angle constant and thus offers zero work. For AW and PAW, the sum of work exerted by the shoulder and wrist joints gives the increased total work, although the work by shoulder joint is smaller than that for NW. The work by gravitational force is almost the same, even though various patterns of wrist actions are employed. Table 2-2 also shows that the ratio of the club head kinetic energy to total work is enhanced for PW, AW and PAW. This means that the efficiency of the swing is improved, especially for AW and PAW where the positive wrist torque is used.

Through analyzing the energy transference from the input joints of shoulder and wrist to club head, we find that two factors determine the club head speed at impact: (1) the work produced by the golfer; and (2) the efficiency index of swing motion η.It is evident that the larger the two factors are, the faster the club head speed at impact is. For the wrist action using the positive torque (AW and PAW), both factors are enhanced as compared with those for NW, and thus the improvement of club head speed at impact can be achieved.

Table 2-3. Comparison of work and kinetic energy at impact between two criteria (J).The results in this table are obtained by which values from the maximum criterion minus those from the impact criterion.

Work and energy	NW	PW with 15 Nm	AW with 15 Nm	PAW with 15 Nm
Total work	0.14	0.71	1.68	1.62
Work by shoulder joint	0.15	0.19	1.44	1.39
Work by wrist joint	0	0	0.31	0.32
Work by gravity	-0.01	0.52	-0.07	-0.09
Kinetic energy of arm	0.02	0	0.24	-0.02
Kinetic energy of club head	0.09	0.14	1.14	1.31

Table 2-3 shows the comparison of the work and kinetic energy between the two criteria. It can be observed that a very small distinction is found, which means that for the two criteria, the energy flowing into the swing system and the energy distributing at impact are almost the same. Thus the club head speeds at impact are highly close for the two criteria.

It should be noted that the values of maximal horizontal club head speed and optimum ball position are obviously affected by different values of model parameters and initial conditions. To examine the influence of small changes in model parameter values on the above results, the equations of motion of golf swing are re-written in another pattern [1].

$$\begin{aligned}&\left(SMA + SMC + MC\,LA^2 + 2\,FMC\,LA\,Cos\,\theta_2\right)\ddot{\theta}_1 + \left(SMC + FMC\,LA\,Cos\,\theta_2\right)\ddot{\theta}_2 \\ &-\left(2\,\dot{\theta}_1 + \dot{\theta}_2\right)FMC\,LA\,Sin\,\theta_2\,\dot{\theta}_2 \\ &+ g\,Sin(IP)\left(FMC\,Cos\left(\vartheta_1 + \theta_2\right) + \left(FMA + MC\,LA\right)Cos\,\theta_1\right) = G_1\end{aligned} \tag{2-20}$$

$$\begin{aligned}&\left(SMC + FMC\,LA\,Cos\,\theta_2\right)\ddot{\theta}_1 + SMC\,\ddot{\theta}_2 + FMC\,LA\,Sin\,\theta_2\,\dot{\theta}_1^2 \\ &+ g\,Sin(IP)\,FMC\,Cos\left(\vartheta_1 + \theta_2\right) = G_2\end{aligned} \tag{2-21}$$

Where seven new parameters are denoted as: SMA = second moment of arm about shoulder joint (I); FMA = first moment of arm about shoulder joint (m_1l_1); LA =length of arm (a_1); SMC = second moment of club about wrist joint ($J+m_2l_2^2$); FMC = first moment of club about wrist joint (m_2l_2); MC =mass of club (m_2); IP =Inclination of plane of downswing (ϕ)

The maximal horizontal club head speed and optimum ball position are investigated again by the two criteria, with increasing only one parameter such as SMA by ten percent and maintaining the others at their original values.

The numerical results demonstrate that both the maximal horizontal club head speed and optimum ball position change slightly with the ten percent increases in parameter values. For example, when 15 Nm wrist torque is used, the maximal changes in club head speed and ball position are no more than 1.2913 m/s (2.6 % as compared to the original) and 78 mm, respectively. It is of great interest that the impact criterion can still determine

the optimum ball position, even though the relative model parameter values are increased by ten percent (Table 2-4). It is fairly clear that the differences in club head speed and ball position between the two criteria are very small for all the seven increased parameters. For NW, the maximal difference in speed is merely 0.0002 m/s; and the maximal distinction in ball position is only 4mm. For PW, the maximal differences in speed and ball position are 0.0004 m/s and 6mm, respectively. For AW and PAW, the relatively large differences are exhibited, but can not influence the effectiveness of impact criterion because the maximal distinction in club head speed (0.0279 m/s) is no more than 0.057%, as compared to that by the maximum criterion.

Table 2-4. Comparison between two criteria with a varied model parameter (15 Nm wrist torque is used)

	SMC	FMC	MC	SMA	FMA	LA	IP
Original parameter values	0.3004 $kg.m^2$	0.2967 kg.m	0.3940 kg	1.1500 $kg.m^2$	2.3837 kg.m	0.6150 m	60.0000 deg
Parameter changes (percent)	10	10	10	10	10	10	10
Difference in club head speed (m/s)	0.0001(NW) 0 (PW) 0.0215(AW) 0.0204(PAW)	0 (NW) 0.0003 (PW) 0.0228 (AW) 0.0241 (PAW)	0.0002 (NW) 0.0004 (PW) 0.0263 (AW) 0.0263 (PAW)	0.0002 (NW) 0.0004 (PW) 0.0279 (AW) 0.0278 (PAW)	0.0002 (NW) 0.0004 (PW) 0.0258 (AW) 0.0258 (PAW)	0 (NW) 0.0001 (PW) 0.0244(AW) 0.0243 (PAW)	0.0002 (NW) 0.0004 (PW) 0.0259 (AW) 0.0259 (PAW)
Difference in ball position (mm)	0 (NW) 0 (PW) 42 (AW) 40 (PAW)	2 (NW) 5 (PW) 42 (AW) 42 (PAW)	4 (NW) 5 (PW) 46 (AW) 44 (PAW)	4 (NW) 6 (PW) 47 (AW) 47 (PAW)	4 (NW) 5 (PW) 47 (AW) 44 (PAW)	1 (NW) 3 (PW) 44 (AW) 44 (PAW)	4 (NW) 5 (PW) 47 (AW) 44 (PAW)

The same procedures are repeated, when the initial angles of the arm and club are changed by ten percent, respectively ($\theta_1(0)=99^\circ$ or $\theta_2(0)=-99^\circ$). Similar results are observed: the maximal changes in club head speed and ball position are no more than 1.1746 m/s (2.5 % as compared to the original) and 35 mm, respectively; the maximal distinction in club head speed between the two criteria is only 0.0282 m/s.

We should also note that the simulation results, including maximum club head speed and optimum ball position, depend on what is fed into the downswing model. So far the simulation has been mainly concerned with constant torque pattern. Different torque patterns are also used in the calculation. For example, the shoulder torque is applied as a ramp function with rise time 110 ms and maximum magnitude 110 Nm, and the positive wrist toque is increased linearly in time from 0 with a constant slope of 93.7 Nm/s (the maximum wrist torque is 15 Nm). The results show very much the same as for the constant torque pattern: the impact criterion still works well for various types of wrist actions to determine the optimum ball position (the maximal distinction in club head speed is only 0.0277 m/s between the two criteria); PAW gives the highest club head speed as compared to NW, PW and AW; the positive wrist torque enhances both factors in determining the club head speed.

2.6 Summary

The purpose of this chapter is to examine whether the combination of ball position and wrist action (different types of torque applications) can increase the horizontal club head speed at impact. A 2-dimentional double-pendulum model of golf downswing is used to determine what extent wrist action increases the club head speed in a driver, and affects the optimum ball position. Three different patterns of wrist actions (negative,

positive, and negative-positive torque at the wrist) are investigated; and two optimization methods (maximum and impact criteria) used to assess their effectiveness - maximum horizontal club head speed and club head speed as the shaft becomes vertical when viewed 'face-on'. The simulation results indicate that the horizontal club head speed at impact can be increased by these patterns of wrist actions, and the optimum ball position can be determined by the impact criterion. Based on the analysis of the energy flow from the input joints of shoulder and wrist to the arm and club head, we discuss the way the wrist action affects the club head speed. The sensitivity of the results to small changes in model parameter values and initial conditions is investigated. The results are also examined under different torque patterns.

Chapter 3

Study on the wrist action in a new swing model

3.1 Mathematical model

The dynamic model of golf swing is shown in Figure 3-1. The rotations of the arm and golf club are assumed to occur in one plane during the downswing and follow-through, and this plane is inclined with an angle θ to the ground. The assumption of the planar movement of the arm and golf club is well supported in the early work of Cochran & Stobbs [2] and Jorgensen [1]. Therefore, the gravity acceleration vector in the swing plane is expressed as $\boldsymbol{g} = \begin{bmatrix} 0 & -g_0 \end{bmatrix}^T$, $g_0 = g\,Sin\theta$. In our model, the arm and golf grip are considered as the rigid rods, the club head as a tip mass and golf shaft is treated as an Euler-Bernoulli beam. Two co-ordinate systems in the swing plane are introduced to describe the dynamics of the golf swing: a fixed reference frame *XY*; and a rotational reference frame *xy* that attached to the end of golf grip, where its *x*-axis is along the undeformed configuration of golf shaft. Since the center of gravity of club head is regarded as on the central axis of golf shaft, the twisting of golf shaft is neglected and the bending flexibility of golf shaft in the swing plane is only considered. Due to the rotational motion of the system, golf shaft is stiffened by an axial force [17]. The centrifugal stiffening of golf shaft is thus taken into account in this study.

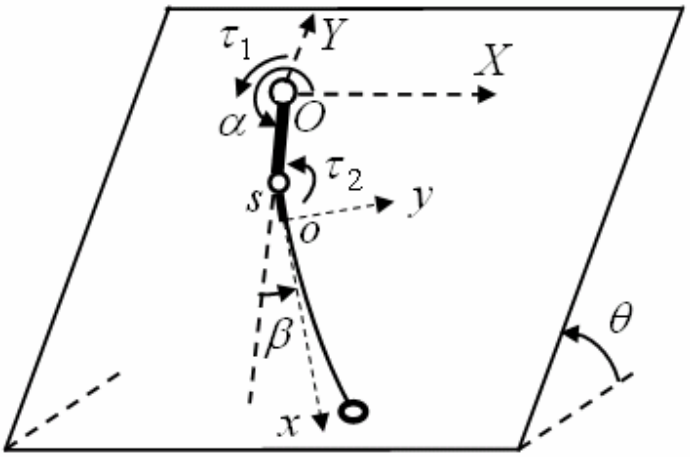

Figure 3-1 Dynamic model of golf swing. The torque τ_1 is applied at the shoulder joint O to drive the swing; the torque τ_2 is employed at the wrist joint s to hold golf club. The rotational arm angle is α, and the club angle is β.

The Euler-Lagrange approach is used to derive the dynamic equations of motion for a golfer's swing. In the co-ordinate system $O-XY$, $\boldsymbol{r}_2$ and $\boldsymbol{r}_R$ are the position vectors of the centers of gravity of golf grip and club head, respectively; $\boldsymbol{r}_p$ is the position vector of a point p on the shaft; y_p is the bending displacement of a point p on the shaft in the co-ordinate system *o-xy*; J_1 is the moment of inertia of arm about the shoulder joint *O*; J_2 and J_R are the moments of inertia of golf grip and club head, respectively; m_1, m_2, m_3 and m_R are the masses of arm, golf grip, golf shaft and club head, respectively; a_1, a_2 and a_3 are the lengths of arm, golf grip and shaft, respectively; R is the radius of club head; ρ is the mass per unit length of golf shaft; E is the Young's modulus of golf shaft material; I is the area moment of inertia of golf shaft.

The following operators are denoted

$$\dot{(*)} \equiv \frac{\partial}{\partial t}(*) \quad \text{and} \quad (*)' \equiv \frac{\partial}{\partial x}(*)$$

The total kinetic energy of the system is given by

$$T = T_1 + T_2 + T_3 + T_4 . \tag{3-1}$$

where T_1, T_2, T_3 and T_4 are the kinetic energy associated with arm, golf grip, golf shaft and club head , respectively. They are

$$T_1 = \frac{1}{2} J_1 \dot{\alpha}^2 . \tag{3-2}$$

$$T_2 = \frac{1}{2} J_2 \left(\dot{\alpha} + \dot{\beta}\right)^2 + \frac{1}{2} m_2 \, \dot{\boldsymbol{r}}_2^T \dot{\boldsymbol{r}}_2 . \tag{3-3}$$

$$T_3 = \frac{1}{2} \rho \int_0^{a_3} \dot{\boldsymbol{r}}_p^T \; \dot{\boldsymbol{r}}_p \, dx . \tag{3-4}$$

$$T_4 = \frac{1}{2} m_R \, \dot{\boldsymbol{r}}_R^T \dot{\boldsymbol{r}}_R + \frac{1}{2} J_R \left(\dot{\alpha} + \dot{\beta} + \dot{y}' \Big|_{x=a_3} \right)^2 . \tag{3-5}$$

The potential energy resulting from the gravitational forces on arm and golf grip are

$$U_1 = -m_1 \, \boldsymbol{g}^T \boldsymbol{r}_1 . \tag{3-6}$$

$$U_2 = -m_2 \, \boldsymbol{g}^T \boldsymbol{r}_2 . \tag{3-7}$$

The potential energy of golf shaft is written as

$$U_3 = U_{31} + U_{32} + U_{33} . \tag{3-8}$$

where

$$U_{31} = \frac{1}{2} EI \int_0^{a_3} \left(y_p'' \right)^2 dx. \tag{3-9}$$

$$U_{32} = -\rho \, \boldsymbol{g}^T \int_0^{a_3} \boldsymbol{r}_p \, dx. \tag{3-10}$$

U_{31} and U_{32} are the potential energy due to the elastic deformation and gravitational force for golf shaft, respectively.

The axial force, resulting from the axial centripetal accelerations of golf shaft and club head, causes the potential energy U_{33} .

$$U_{33} = \frac{1}{2}\int_0^{a_3} f_x^p \left(y_p'\right)^2 \, dx \tag{3-11}$$

where

$$f_x^p = f_{x1}^p + f_{x2}^p \tag{3-12}$$

f_x^p is the axial force for a point p on golf shaft; f_{x1}^p, f_{x2}^p are the axial forces for the point p, resulting from the axial centripetal accelerations of golf shaft and club head, respectively. They are

$$f_{x1}^p = -\rho \int_x^{a_3} A_{x1}^p \, dx \tag{3-13}$$

$$f_{x2}^p = -m_R \, A_{x2}^{tip} \tag{3-14}$$

where A_{x1}^p and A_{x2}^{tip} are the axial accelerations for the point p and club head, respectively; both of them are directed along the x-axis.

The specific expressions of f_{x1}^p is given by

$$f_{x1}^p = \frac{1}{2}(a_3 - x)\rho \begin{pmatrix} (2a_2 + a_3 + x + 2a_1 \, Cos(\beta))\dot{\alpha}^2 \\ +2(2a_2 + a_3 + x)\dot{\alpha}\,\dot{\beta} + (2a_2 + a_3 + x)\dot{\beta}^2 - 2a_1 Sin(\beta)\ddot{\alpha} \end{pmatrix} \tag{3-15}$$

It should be noted that the terms associated with the deformation of golf shaft y_p have been ignored since the potential energy resulting from them is relatively small as compared to the other terms.

The potential energy due to the gravitational force for club head is

$$U_4 = -m_R \, \boldsymbol{g}^T \boldsymbol{r}_R . \tag{3-16}$$

The total potential energy of this system can be written as

$$U = U_1 + U_2 + U_3 + U_4 . \tag{3-17}$$

The Lagrangian L of the system can be obtained as

$$L = T - U\,. \tag{3-18}$$

It is also noted that the internal structural damping in golf shaft should be considered. By using Rayleigh's dissipation function, the dissipation energy for golf shaft is written as

$$E_D = \sum_{i=1}^{m} \frac{1}{2} d_i \dot{q}_i^2 \tag{3-19}$$

where d_i and q_i are the damping coefficient and mode amplitude associated with the *i*th mode of golf shaft bending vibration, respectively.

According to the assumed modes technique in Theodore & Ghosal [18], a finite-dimensional model of golf shaft bending displacement is written as

$$y(x,t) = \sum_{i=1}^{m} \phi_i(x) q_i(t) \tag{3-20}$$

Where $\phi_i(x)$ and $q_i(t)$ are the *i*th assumed mode eigen function and time-varying mode amplitude, respectively. As the shaft is modeled as an Euler-Bernoulli beam with uniform density and constant flexural rigidity (*EI*), it satisfies with the following partial differential equation

$$EI \frac{\partial^4 y(x,t)}{\partial x^4} + \rho \frac{\partial^2 y(x,t)}{\partial t^2} = 0 \tag{3-21}$$

we can obtain the general solution of Eq. 3-21:

$$q_i(t) = \exp(j\, w_i t). \tag{3-22}$$

where w_i is the *i*th natural angular frequency.

Furthermore, $\phi_i(x)$ can be expressed as

$$\phi_i(x) = C_{1i}\, sin(\varepsilon_i\, x) + C_{2i} cos(\varepsilon_i\, x) + C_{3i} sinh(\varepsilon_i\, x) + C_{4i} cosh(\varepsilon_i\, x) \tag{3-23}$$

where $\varepsilon_i^4 = \dfrac{w_i^2\, \rho}{EI}$

The golf club has been considered as a cantilever that has a tip mass, so the following 4 expressions associated with the boundary conditions can be obtained [19].

$$y\big|_{x=0} = 0\,. \tag{3-24}$$

$$y'\big|_{x=0} = 0\,. \tag{3-25}$$

$$EI\, y''\big|_{x=a3} = -\left(J_R + m_R\, R^2\right) \ddot{y}'\big|_{x=a3}\,. \tag{3-26}$$

$$EI\, y'''\big|_{x=a3} = m_R\, \ddot{y}\big|_{x=a3}\,. \tag{3-27}$$

From these boundary conditions, the following results are given

$$C_{1i} = -C_{3i} \quad \text{and} \quad C_{2i} = -C_{4i}\,. \tag{3-28}$$

$$\begin{bmatrix} A_{11} & A_{12} \\ A_{21} & A_{22} \end{bmatrix} \begin{bmatrix} C_{1i} \\ C_{2i} \end{bmatrix} = 0\,. \tag{3-29}$$

The *i*th natural angular frequency w_i can be obtained by solving the eigenvalue problem of the matrix equation (3-29), and the coefficients C_{1i} and C_{2i} are chosen by normalizing the mode eigen functions $\phi_i(x)$ such that

$$\rho \int_0^{a_3} \phi_i^2(x)\, dx = m_3\,, \quad i = 1, 2 \cdots m\,. \tag{3-30}$$

On the basis of the Euler-Lagrange equation

$$\frac{\partial}{\partial t}\left(\frac{\partial L}{\partial \dot{Q}_i}\right) - \frac{\partial L}{\partial Q_i} + \frac{\partial E_D}{\partial \dot{Q}_i} = f_i \tag{3-31}$$

with the Lagrangian *L*, the dissipation energy of golf shaft E_D, the generalized coordinates Q_i and the corresponding generalized forces f_i, the dynamic equations of motion of golf swing are achieved. Since the amplitudes of the lower modes of golf shaft bending vibration are apparently larger than those of the higher modes, *m* is simplified to

two in this study.

The equations of motion of golf swing can be written as.

$$\boldsymbol{B}(\theta)\ddot{\theta}+\boldsymbol{h}(\theta,\dot{\theta})+\boldsymbol{K}\theta+\boldsymbol{G}(\theta)+\boldsymbol{D}\dot{\theta}=\boldsymbol{\tau} \tag{3-32}$$

Where

$$\boldsymbol{B}=\begin{bmatrix} B_{11} & B_{12} & B_{13} & B_{14} \\ B_{21} & B_{22} & B_{23} & B_{24} \\ B_{31} & B_{32} & B_{33} & B_{34} \\ B_{41} & B_{42} & B_{43} & B_{44} \end{bmatrix}, \boldsymbol{\theta}=\begin{bmatrix} \alpha \\ \beta \\ q_1 \\ q_2 \end{bmatrix}, \boldsymbol{h}=\begin{bmatrix} h_1 \\ h_2 \\ h_3 \\ h_4 \end{bmatrix}, \boldsymbol{K}=\begin{bmatrix} 0 & 0 & 0 & 0 \\ 0 & 0 & 0 & 0 \\ 0 & 0 & K_{33} & K_{34} \\ 0 & 0 & K_{34} & K_{44} \end{bmatrix}$$

$$\boldsymbol{G}=\begin{bmatrix} G_1 \\ G_2 \\ G_3 \\ G_4 \end{bmatrix}, \boldsymbol{D}=\begin{bmatrix} 0 & 0 & 0 & 0 \\ 0 & 0 & 0 & 0 \\ 0 & 0 & d_1 & 0 \\ 0 & 0 & 0 & d_2 \end{bmatrix}, \boldsymbol{\tau}=\begin{bmatrix} \tau_1 \\ \tau_2 \\ 0 \\ 0 \end{bmatrix}$$

$\boldsymbol{B}$, $\boldsymbol{K}$ and $\boldsymbol{D}$ are the inertia, stiffness and damping matrices, respectively; $\boldsymbol{h}$ is the nonlinear force vector; $\boldsymbol{G}$ is the gravity vector and $\boldsymbol{\tau}$ is the input vector; q_1 and q_2 are the first and second time-varying mode amplitudes of the shaft bending vibration, respectively; d_1 and d_2 are the damping coefficients of the first and second modes of the shaft bending vibration, respectively.

3.2 Optimization method

Based on the above part (3.1 Mathematical model), the bending displacement of club head, y_c, is given by

$$y_c=\phi_1(a_3)q_1(t)+\phi_2(a_3)q_2(t) \tag{3-33}$$

Where $\phi_1(a_3)$ and $\phi_2(a_3)$ are the first and second mode shape functions of bending vibration for the end of golf shaft, respectively.

The horizontal component of club head velocity, v_h, is written as

$$v_h = -a_1 \,\boldsymbol{sin}\,\alpha\,\dot{\alpha} - (a_2 + a_3 + R)\,\boldsymbol{sin}(\alpha+\beta)(\dot{\alpha}+\dot{\beta}) - \dot{y}_c\,\boldsymbol{sin}(\alpha+\beta) - y_c\,\boldsymbol{cos}(\alpha+\beta)(\dot{\alpha}+\dot{\beta}) \tag{3-34}$$

Substituting Eq.(3-33) into Eq.(3-34), and then differentiating the result with respect to time, it is found that v_h will reach a maximal value when

$$\begin{aligned} &-a_1\left(\boldsymbol{cos}\,\alpha\,\dot{\alpha}^2 + \boldsymbol{sin}\,\alpha\,\ddot{\alpha}\right) - (a_2 + a_3 + R)\left(\boldsymbol{cos}(\alpha+\beta)(\dot{\alpha}+\dot{\beta})^2 + \boldsymbol{sin}(\alpha+\beta)(\ddot{\alpha}+\ddot{\beta})\right) \\ &\quad -(\phi_1(a_3)\ddot{q}_1 + \phi_2(a_3)\ddot{q}_2)\,\boldsymbol{sin}(\alpha+\beta) - 2(\phi_1(a_3)\dot{q}_1 + \phi_2(a_3)\dot{q}_2)\,\boldsymbol{cos}(\alpha+\beta)(\dot{\alpha}+\dot{\beta}) \\ &\quad +(\phi_1(a_3)q_1 + \phi_2(a_3)q_2)\left(\boldsymbol{sin}(\alpha+\beta)(\dot{\alpha}+\dot{\beta})^2 - \boldsymbol{cos}(\alpha+\beta)(\ddot{\alpha}+\ddot{\beta})\right) = 0 \end{aligned} \tag{3-35}$$

The fourth-order Runge-Kutta method at intervals of 1.0×10^{-5} s was used to solve Eq. (3-32), and the left-side expression of Eq. (3-35) was evaluated at each time-step. The optimum time t_o, at which the horizontal club head velocity arrives at a maximal value, was achieved when the left-side expression of Eq. (3-35) is most close to zero. Then the corresponding values of $\alpha, \beta, \dot{\alpha}, \dot{\beta}, y_c$ and $\dot{y}_c$ at t_o could be calculated. The optimum ball position, p_h, is also calculated at t_o:

$$p_h = a_1\,\boldsymbol{cos}\,\alpha + (a_2 + a_3 + R)\,\boldsymbol{cos}(\alpha+\beta) - y_c\,\boldsymbol{sin}(\alpha+\beta) \tag{3-36}$$

3.3 Wrist action simulation

Both Jorgensen [1] and Sprigings & Neal [9] have suggested that the optimal 'timing' of the activation of positive wrist torque occurred when the left arm was about 30° below the horizontal line through the shoulder joint ($\alpha = 210^\circ$ in this chapter). This conclusion is also consistent with the result obtained from Chapter 2. Therefore, the neutral and positive wrist torques, activated from the optimal 'timing' mentioned above, are used to re-examine whether the club head speed could be improved by means of the

optimization method (maximum horizontal club head speed at impact). In the present study, the positive wrist torque is not constant but increased linearly with time from 0 to 8 Nm, as muscles could not be activated to their full torque magnitude instantaneously.

3.4 Experiment

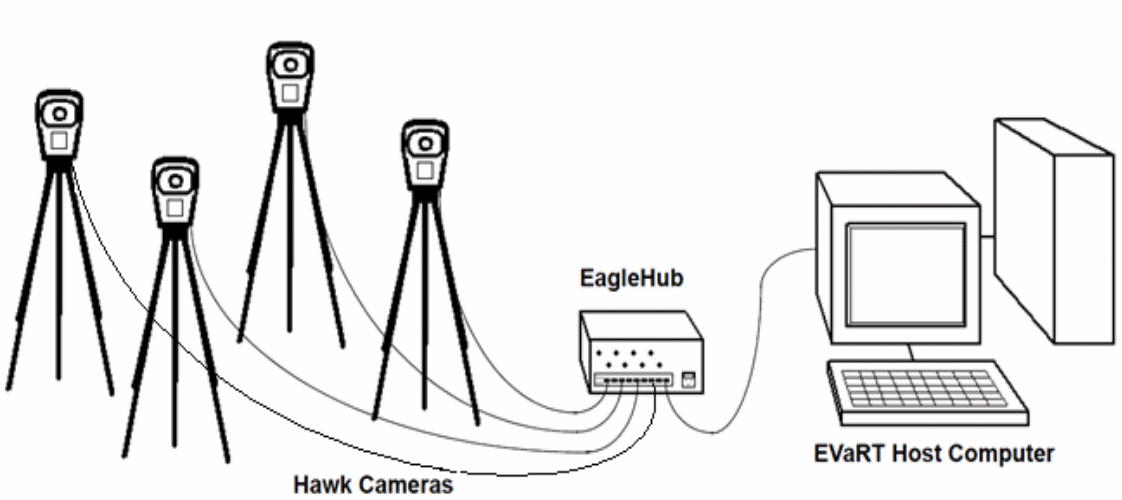

Figure 3-2 Configuration of motion analysis system.

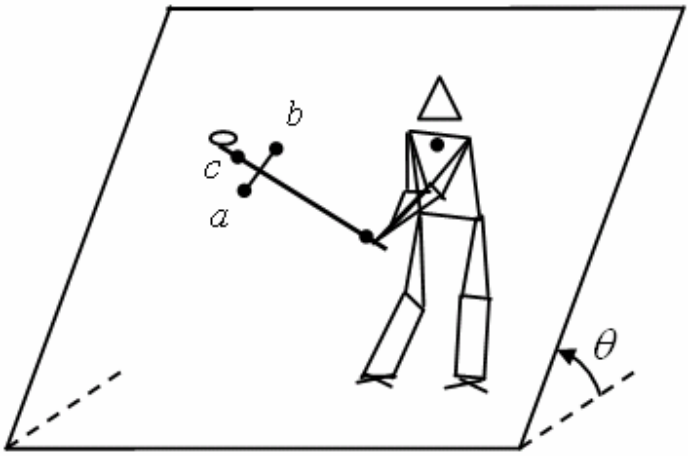

Figure 3-3 Position distribution of the five reflective markers.

Two amateur golfers were analyzed in the experiment. Both subjects were right-handed and labelled as A and B, with handicaps of 10 and 28, respectively. The golf

club used for the experiment was a wooden-clubhead driver with titanium alloy shaft (351 g in mass and 110 cm in length). The swing motions of the subjects' arms and golf club were recorded by a 3-D motion analysis system (MotionAnalysis EVaRT 4.6) with 4 digital cameras (Hawk camera) at a rate of 200 frames per second and shutter speed of 1000 us（Figure 3-2）. Five reflective markers were placed on the subjects and golf club. The specific position distribution of the reflective markers is shown in Figure 3-3. One marker was placed on the center point between the shoulders as the shoulder joint o ; one marker was put on a place on the grip near the grip end of the club as the wrist joint s ; the third marker c was situated at a place near the end of the golf shaft; the last two markers a and b, with the negligible-mass shaft attaching on the golf shaft, were used to measure the orientation of the club during the downswing. Three groups of foil strain gauges (Kyowa, KFRP-2-120-C1-9L3M2R) were boned to the shaft and each group included 2 single-axial type strain gauges. Two groups of strain gauges were bonded to the shaft near the grip to measure two bending moments, which are parallel and normal to the clubface, respectively. The tension of the shaft was measured by the other group of strain gauges situated at the middle of the shaft. The forces and moments were obtained from the appropriate calibration, applying static loadings for the club as fixing the grip in a cantilever manner. The strain gauge data was recorded from at address to the follow-through at the sampling rate of 500 Hz, and the whole course lasted 6 seconds. The strain gauge data was first transmitted by the strain gauge amplifiers (Kyowa, HSC-20BS) and then fed to a personal computer by an A/D convertor (CONTEC, AD12-16(PCI)). The configuration of the strain data collection system is shown in Figure 3-4.

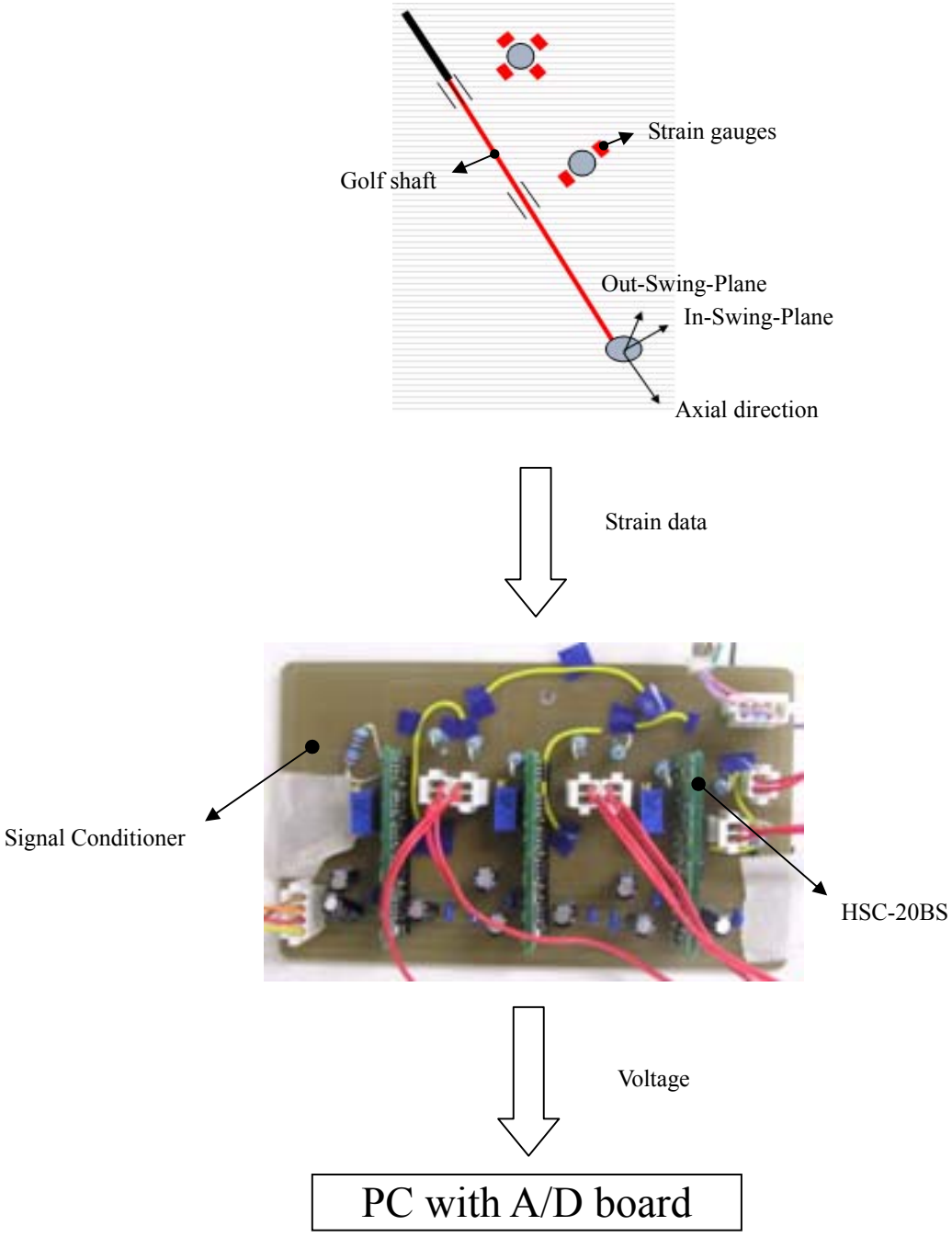

Figure 3-4 Configuration of strain data collection system

As both subjects rotated the club at the latter stage of the downswing to square the clubface at impact, the bending moments, parallel and normal to the clubface, were transformed into two moments: one is in the swing plane and the other in the normal swing plane by the orientation of golf club. This is because that only the in-swing-plane bending moment is considered in our simulation model. It is clear that the wrist torque could be achieved from the measured bending moments near the grip; and the shoulder torque could be gained from the measured shaft tension and hand force along the tangential direction to the arm. Parameter values of arm, including mass, center of mass and moment of inertia, were calculated using the formula given by AE et al. [20]; parameter values for the club were obtained by the actual measurement and experiment modal analysis.

Both subjects were asked to swing 5 times after enough practice until they felt comfortable with the test situation. One swing of each subject A and B was just used to give results since other swings of both subjects could not alter their overall swing styles in nature. As the downswing was our focus, the initial time of the downswing, estimated by the camera system, was chosen as 325 ms and 435 ms before impact for subject A and B, respectively. The initial angles and angular velocities of the arm and golf club were estimated by the motion analysis system; the initial bending displacement of golf shaft was gained from the strain gauge measurement.

3.5 Results and discussion

Based on the measured torques, the simplified shoulder and wrist torques were used to drive our dynamic model. The specific measured and simplified torques of the shoulder and wrist are indicated in Figure 3-5. The wrist actions used by both subjects are

obviously the ones using negative torque (Figure 3-5(b) and Figure 3-5(d)). The comparisons of the speed of marker c on the shaft, arm and club rotational angles between the actual swings and computer simulation are given in Figure 3-6. Note that the swing motions from the proposed dynamic model are consistent with those from the actual swings (Figure 3-6). We should also be aware that the simplified torques applied in the simulation, are not expected to agree exactly with those from the measured ones but approximate to them.

(a)

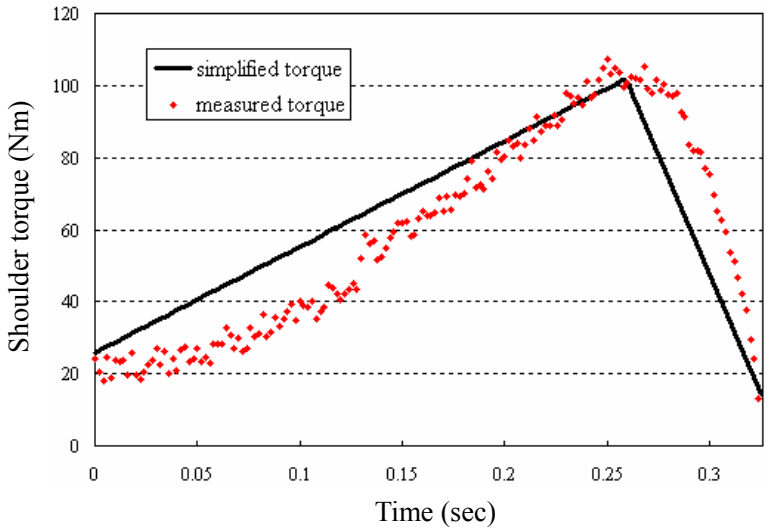

(b)

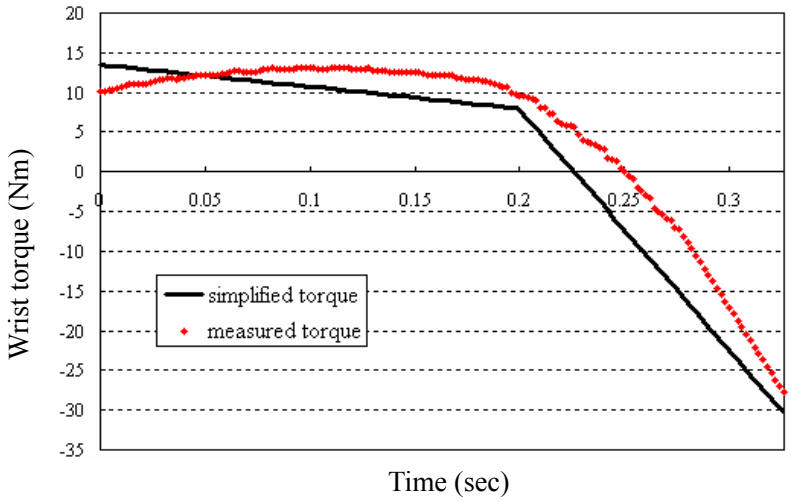

(c)

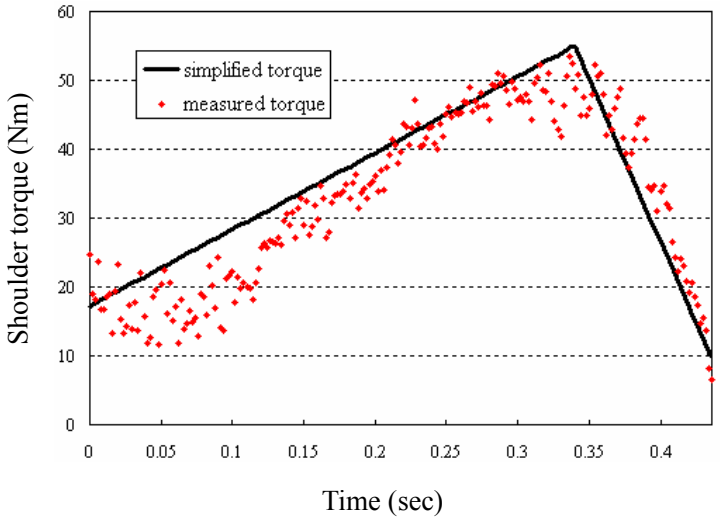

(d)

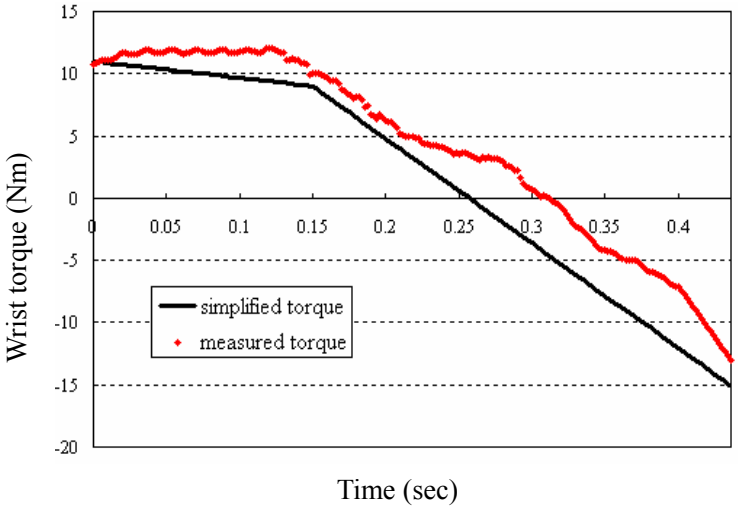

Figure 3-5 Measured and simplified torques for the shoulder and wrist joints. (a) shoulder torque for subject A; (b) wrist torque for subject A; (c) shoulder torque for subject B; (d) wrist torque for subject B;

(a)

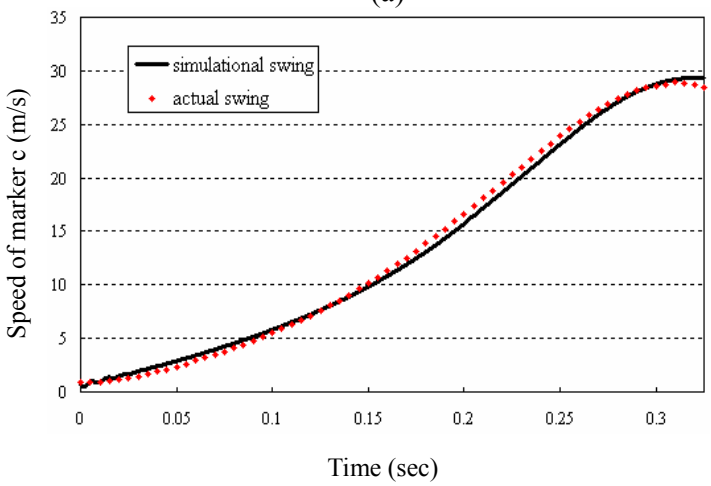
simulational swing
actual swing
Speed of marker c (m/s)
35
30
25
20
15
10
5
0
0
0.05
0.1
0.15
0.2
0.25
0.3
Time (sec)

(b)

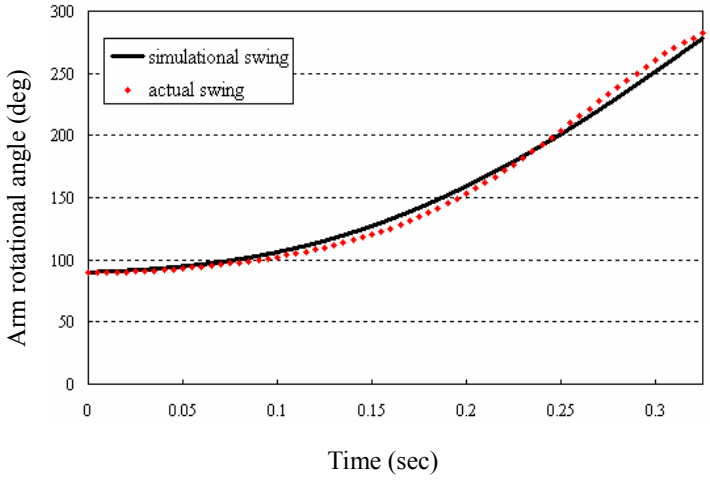
simulational swing
actual swing
Arm rotational angle (deg)
300
250
200
150
100
50
0
0
0.05
0.1
0.15
0.2
0.25
0.3
Time (sec)

(c)

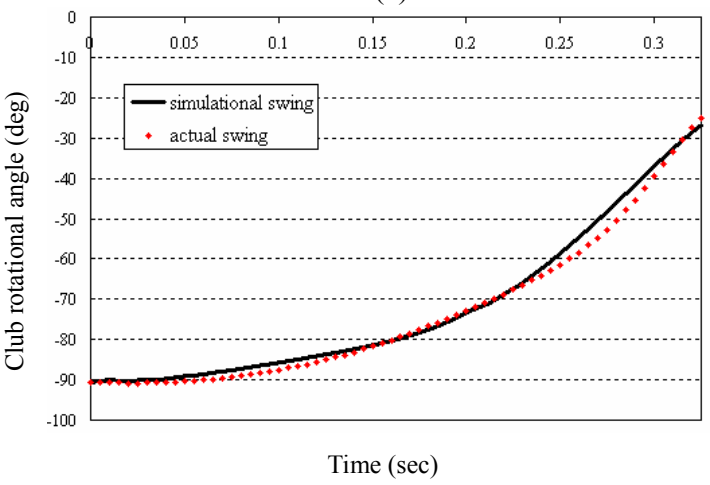
simulational swing
actual swing
Club rotational angle (deg)
0
-10
-20
-30
-40
-50
-60
-70
-80
-90
-100
0
0.05
0.1
0.15
0.2
0.25
0.3
Time (sec)

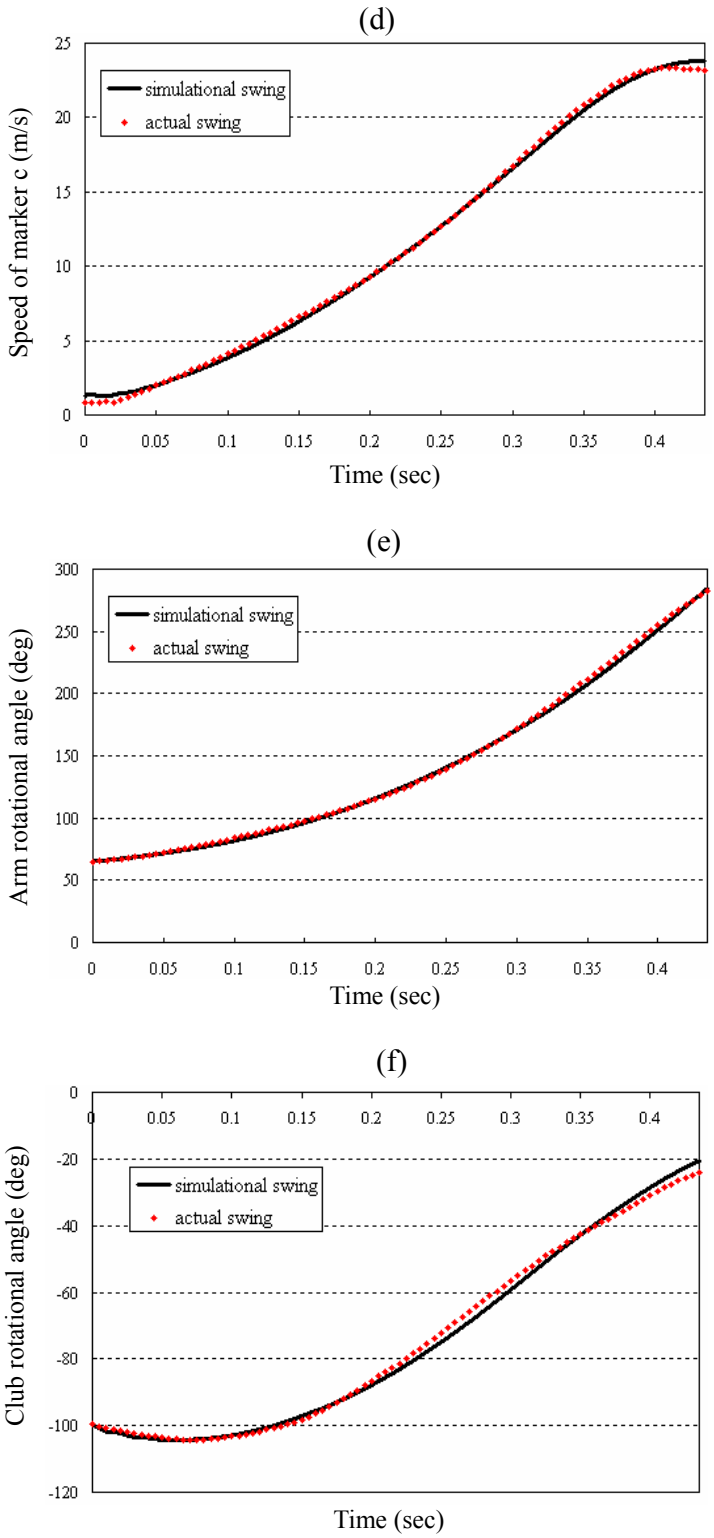

Figure 3-6 Comparisons of speed of marker c on the shaft, arm and club rotational angles obtained from the actual swing and computer simulation. (a) speed of marker c for subject A; (b) arm rotational angle for

subject A; (c) club rotational angle for subject A; (d) speed of marker c for subject B; (e) arm rotational angle for subject B; (f) club rotational angle for subject B.

The maximum horizontal club head speed at impact using three patterns of wrist actions are indicated in figure 3-7. It can be seen that the positive wrist torque results in the maximum club head speed at impact, 40.40 m/s for subject A and 32.18 m/s for subject B, giving the corresponding increases by 13.7 % and 12.0 % when compared with those using negative torque. The neutral wrist torque also provides an improvement in club head speed, and the increases are 11.0 % and 8.2 % for subject A and B, respectively.

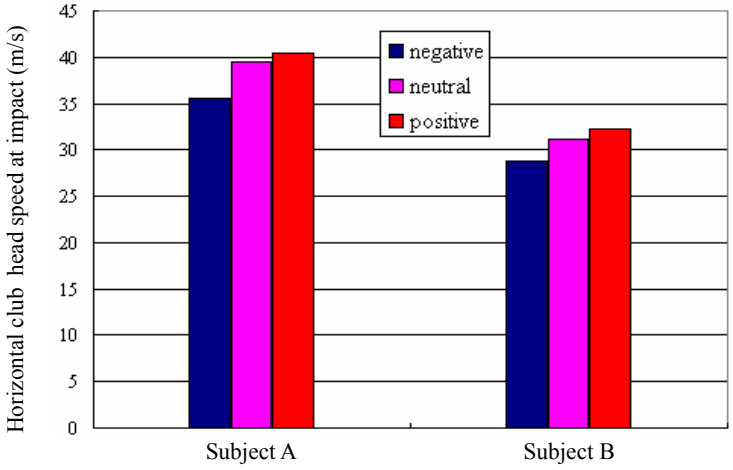

Figure 3-7 Maximum horizontal club head speed at impact using different wrist actions

The optimum ball position at impact is shown in Figure 3-8. We can see that the optimum ball position is different for the various types of wrist actions. However, for both subjects the positive torque gives the largest optimum ball position, followed by the neutral torque, followed by the negative torque.

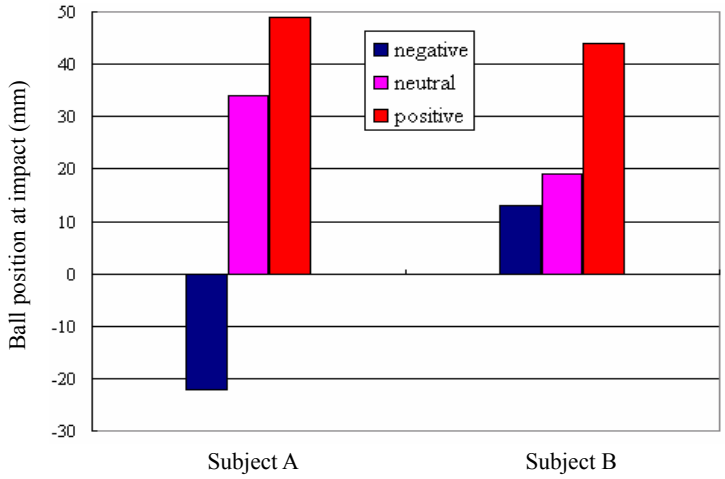

Figure 3-8 Optimum ball position at impact using different wrist actions

An energy based analysis method, the same one as shown in Chapter 2, with the ball position inconstant but being optimally determined (Maximum criterion), is used to search for how the wrist action affects the club head speed. Figure 3-9 shows the total work exerted by a golfer using three kinds of wrist actions. The application of the positive wrist torque leads to the maximum total work, and the negative gives the minimum. It should be noticed that the club head speed at impact is determined not only by the total work produced by a golfer but also by how the resulting energy delivers from the arm to club head. Figure 3-10 shows the efficiency index of swing motion η. It is shown that the positive wrist torque yields the maximum value of η, 75.4 % for subject A and 77.5 % for subject B. This phenomenon may be explained by that the positive wrist torque causes the high club angular speed, which in turn results in the large centrifugal force of golf club to retard the arm, so the arm angular speed is decreased, and as a result, the efficiency index η is increased. This point is consistent with the opinion in the work of Budney & Bellow [4], in which a positive wrist torque instead of a retarding torque was used to enhance the club head speed on condition of a reduced arm angular speed.

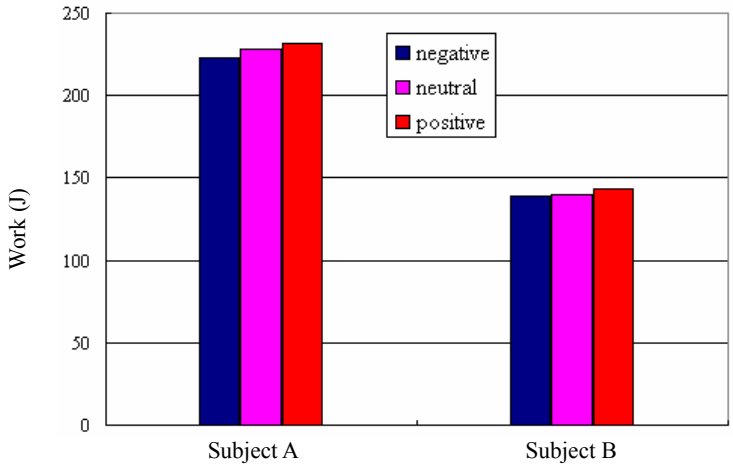

Figure 3-9 Total work generated by golfers using different wrist actions.

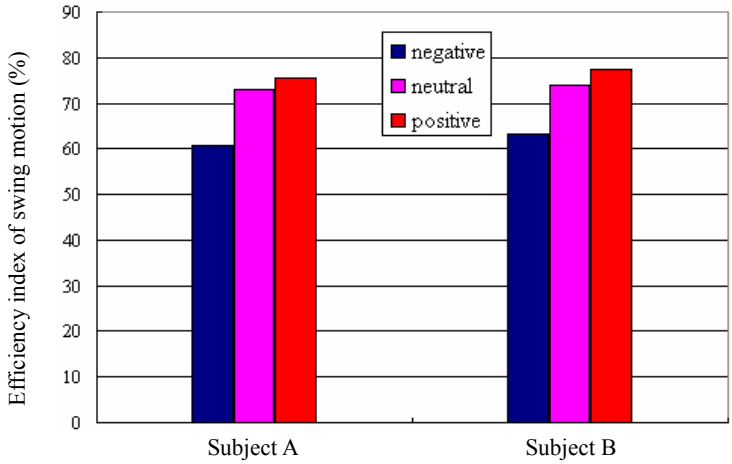

Figure 3-10 Efficiency index of swing motion using different wrist actions

It can be seen that the ‘absorbed’ or ‘released’ bending strain energy of golf shaft at impact is exhibited to be different for various patterns of wrist actions (Figure 3-11). The negative wrist torque indicates the maximum ‘absorbed’ strain energy, 1.06 J for subject A .The neutral wrist torque, however, gives the maximum ‘released’ strain energy, -0.40 J for subject A and -0.45 J for subject B, which can be transformed into the kinetic energy of clubhead and thus the speed is increased. The positive wrist torque also offers

the ‘released’ strain energy, but the values, -0.31 J for subject A and -0.35 J for subject B, are smaller than those using neutral torque.

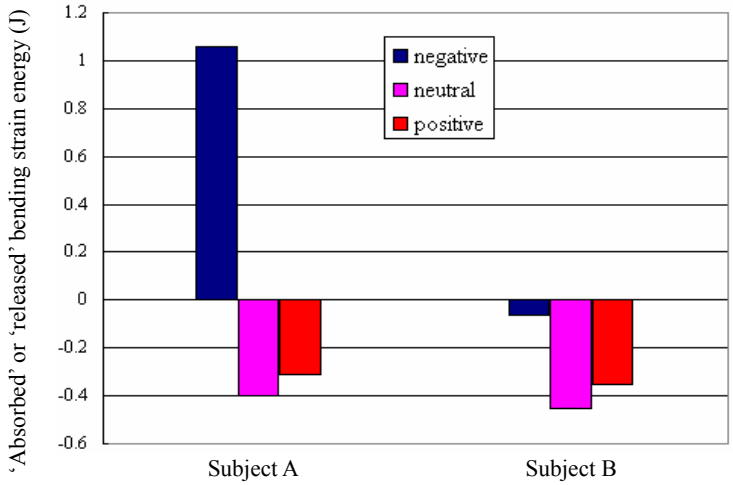

Figure 11 ‘Absorbed’ or ‘released’ bending strain energy of golf shaft at impact. The value is calculated as the bending strain energy at impact minus that at the initial. The positive value is defined as ‘absorbed’; the negative value is denoted as ‘released’

The main purpose of this study was to examine whether different wrist actions in consideration of ball position offer a benefit to horizontal club head speed at impact by a new golf swing model. Considering the bending flexibility and centrifugal stiffening of golf shaft, a two-dimensional dynamic model, derived from a combined Euler-Lagrange formulation and assumed mode technique, was used to emulate the downward phase of golf swing. Although the torques of shoulder and wrist employed in this model are not exactly the same as those by the measurements, they are relatively close to the actual ones with necessary simplifications. Moreover, it is the good agreement of swing motions, including the speed of marker c on the shaft, arm and club rotational angles, between the actual swings and computer simulation for both subjects that leads to considerable confidence in the verity of the proposed dynamic model.

The simulation results show that the positive wrist torque, activated at the optimum 'timing' ($\alpha = 210^\circ$), provides a significant gain in club head speed when compared with those using negative wrist torque (13.7% for subject A and 12.0% for subject B). But a relatively small improvement in speed is achieved as compared to those using neutral wrist torque (2.5% for subject A and 3.5% for subject B). This finding agrees with the results from Jorgensen [1] (0.7 %) and Sprigings & Neal [10] (9 %), although the bending flexibility of golf shaft was not included in their models. Note that the percentage gain in club head speed is, however, different with those from their simulation. The most likely reason is that various magnitude of wrist torque was used: the maximum torque is only 2.7 Nm in Jorgensen [1], but 18.5 Nm in Sprigings & Neal [10] and 8.0 Nm in the present study.

Pickering & Vickers [11], using a two-rigid-segment model of golf swing, made an attempt to determine the optimum ball position for golfers using negative wrist torque (the so-called 'late hit'); and found that the optimum ball position should be relatively large. From our simulation results, the optimum ball position is found to be determined by various types of wrist actions. The negative wrist torque, contrary to the conclusion of Pickering & Vickers [11], gives a relatively small optimum ball position, while the positive wrist torque leads to a relatively large optimum ball position instead. This might be attributed to the involvement of the bending vibration of golf shaft in our model, which is neglected in their model.

It is certainly important to know how the wrist action changes the club head speed. Some researchers, including Jorgensen [3] and Sprigings & Mackenzie [9], used a rigid-segment model of golf swing to search for the answer, but the bending flexibility of

golf shaft was not considered in their models; Using a model considering bending vibration of golf shaft, Suzuki & Inooka [12] thought that the properly 'timed' wrist action could effectively utilize the shaft elasticity to improve the club head speed, yet the explicit explanations were not given. Through analyzing the energy transference from the input joints of shoulder and wrist to club head, the simulation results, in which bending vibration of golf shaft is considered, show that two factors facilitate the club head speed at impact: (1) the work produced by a golfer; (2) the energy transference efficiency from the arm to club head. For the positive wrist torque, both factors are higher than those using negative or neutral wrist torques, so the increase in club head speed at impact is achieved.

It is also found that the most effective transformation of bending strain energy of golf shaft into kinetic energy of club head takes place when the neutral wrist torque is used, in which the 'absorbed' strain energy at the initial of the downswing is almost completely released at impact and thus the correspondingly increase in kinetic energy of club head is achieved. This means that the neutral wrist torque can make the best of golf shaft elasticity to improve the club head speed. But the amount of 'released' bending strain energy at impact is a minor percentage of the total work produced by a golfer (0.18 % for subject A and 0.32 % for subject B). Thus, it can be concluded that the proper wrist technique (neutral wrist torque at the latter stage of the downswing) is capable of utilizing the elasticity of golf shaft by releasing the 'absorbed' bending strain energy to improve the club head speed, but the role in speed increase is relatively small as compared to the total work exerted by a golfer.

So far the simulation has been mainly concerned with a golf club. Three other clubs with different flexural rigidity (*EI*) were examined. *EI* was respectively set to be 20, 50 and 70 N.m^2 as compared to the original 33.78 N.m^2. The results show very much the same as for the original club: the maximum difference of optimum ball position among the four clubs is only 28 mm; and the maximum distinction in club head speed is merely 0.54 m/s. This means that the shaft flexibility appears not to be dynamically significant in the golf downswing, which is consistent with the conclusion of Milne & Davis [7].

It should be noticed that the simulation results are based on the swing styles of two amateur players in our experiment. The strong backswing is exhibited in both subjects' swings just like that shown in the work of Cochran & Stobbs [2]. The new model of the golf downswing can be used as a simulation tool to emulate the swing motions of different golfers. The simulation results clearly show that, for golfers, it would be preferable to employ the positive wrist torque at the latter stage of the downswing, rather than apply the neutral wrist torque, though it can utilize the shaft bending elasticity effectively.

3.6 Summary

This chapter uses a new two-dimensional model of golf downswing to examine whether the combination of ball position and wrist action (various patterns of torque applications) can increase the horizontal club head speed at impact. The bending flexibility and centrifugal stiffening of golf shaft are taken into account in this model, which has been verified by the actual golf swings using a three-dimensional motion analysis system and strain gauge measurements. Three different types of wrist actions (negative, neutral, and positive torque at the wrist) are studied by the maximum criterion

(maximum club head speed at impact); and the corresponding optimum ball positions are determined. The results show that the positive wrist torque can give an increased club head speed as compared with the negative and neutral torques. It is also found that the utilization of golf shaft elasticity by a properly 'timed' wrist torque plays a minor role in the improvement of the club head speed. On the basis of the energy transference from the input joints of shoulder and wrist to club head, we discuss the way the wrist action influences club head speed.

Chapter 4

Dynamic interactions between arms and golf clubs

4.1 Mathematical model

The mathematical model of golf downswing is considered as a 2-dimensional double pendulum, which is the same one as that proposed in Chapter 2. For simplicity, we consider the arm link and golf shaft as continuous distribution of mass and the club head as a tip mass. It is also assumed that $m_2 = m_s + m_h$ and $m_h = \frac{2}{3} m_2$. Here, m_s and m_h are the masses of the golf shaft and club head, respectively. Jorgensen [3] considered that the gravity effect upon the motion of a vigorously swung club could be negligible and this effect could be approximately regarded as a small increase in torques applied at the arm and club links, so the effect of gravity is ignored in our calculation. The dynamics of the golf downswing can be described by the following two differential equations:

$$\begin{aligned}&\left(\frac{1}{3}m_1a_1^2+\frac{7}{9}m_2a_2^2+m_2a_1^2+\frac{5}{3}m_2a_1a_2\,\boldsymbol{cos}\,\theta_2\right)\ddot{\theta}_1\\&+\left(\frac{7}{9}m_2a_2^2+\frac{5}{6}m_2a_1a_2\,\boldsymbol{cos}\,\theta_2\right)\ddot{\theta}_2-\frac{5}{3}m_2a_1a_2\,\boldsymbol{sin}\,\theta_2\dot{\theta}_1\dot{\theta}_2\\&-\frac{5}{6}m_2a_1a_2\,\boldsymbol{sin}\,\theta_2\dot{\theta}_2^2=G1.\end{aligned}\tag{4-1}$$

and

$$\left(\frac{7}{9}m_2a_2^2+\frac{5}{6}m_2a_1a_2\,\boldsymbol{cos}\,\theta_2\right)\ddot{\theta}_1+\frac{7}{9}m_2a_2^2\ddot{\theta}_2+\frac{5}{6}m_2a_1a_2\,\boldsymbol{sin}\,\theta_2\dot{\theta}_1^2=G2.\tag{4-2}$$

We assume that there are two groups, named A and B, play golf. Their input torques on the arm links are equivalent ($G1 = 100$ Nm) and the initial conditions for the differential equations are shown as below:

$$\theta_1(0) = 90^\circ,\ \dot{\theta}_1(0) = 0;\quad \theta_2(0) = -90^\circ,\ \dot{\theta}_2(0) = 0.$$

In order to achieve a clear understanding of the interactions between arms and clubs during the downswing, we make an attempt to find a theoretical relationship. The normalized parameters $k_1 (= a_2/a_1)$, $k_2 (= m_2/m_1)$, $k (= G2/G1)$, $G (= G1/m_1 a_1^2)$ and a scaled time $p (= \sqrt{G}t)$ are introduced into Eq. (4-1) and Eq. (4-2), after some manipulations, they yield

$$\left(\frac{1}{3} + \left(\frac{7}{9}k_1^2 + 1\right)k_2 + \frac{5}{3}k_1 k_2 \cos\theta_2\right)\frac{d^2\theta_1}{dp^2} + \left(\frac{7}{9}k_1^2 k_2 + \frac{5}{6}k_1 k_2 \cos\theta_2\right)\frac{d^2\theta_2}{dp^2} - \frac{5}{3}k_1 k_2 \sin\theta_2 \frac{d\theta_1}{dp}\frac{d\theta_2}{dp} - \frac{5}{6}k_1 k_2 \sin\theta_2 \left(\frac{d\theta_2}{dp}\right)^2 = 1. \tag{4-3}$$

and

$$\left(\frac{7}{9}k_1^2 k_2 + \frac{5}{6}k_1 k_2 \cos\theta_2\right)\frac{d^2\theta_1}{dp^2} + \frac{7}{9}k_1^2 k_2 \frac{d^2\theta_2}{dp^2} + \frac{5}{6}k_1 k_2 \sin\theta_2 \left(\frac{d\theta_1}{dp}\right)^2 = k. \tag{4-4}$$

4.2 Results and discussion

The resulting equations are clearly independent of $G1$, but related only to three normalized parameters k_1, k_2 and k while using the five parameters mentioned above. It is assumed that there are three golfers named A1, A2 and A3 in group A, with the same arm mass 5.00 Kg but different arm lengths 0.56 m, 0.65m and 0.74 m respectively, playing golf clubs with the same mass 0.36 Kg and equivalent length ratios of clubs to arms k_1. It is noted that $\theta_1^{(A1)}(t_{A1})$, $\theta_1^{(A2)}(t_{A2})$ and $\theta_1^{(A3)}(t_{A3})$ are related to $G = G^{(A1)}$,

$G = G^{(A2)}$ and $G = G^{(A3)}$, respectively. Here we take golfers A1 and A3 as an example. Considering $k_2 = 0.072$, $G1^{(A1)} = G1^{(A3)}$ and $k_1^{(A1)} = k_1^{(A3)}$, the values of θ_1 and $\dot{\theta}_1$ during the downswing for two golfers are equivalent in terms of the scaled time p. This means that $\theta_1^{(A1)}(t_{A1}) = \theta_1^{(A3)}(t_{A3})$ at times t_{A1} and t_{A3}, which have the correlation of $t_{A1} = t_{A3}\sqrt{G^{(A3)}/G^{(A1)}}$ in terms of the normal time t. Since $G^{(A1)} = G1^{(A1)}/\left(m_1^{(A1)}\left(a_1^{(A1)}\right)^2\right)$, $G^{(A3)} = G1^{(A3)}/\left(m_1^{(A3)}\left(a_1^{(A3)}\right)^2\right)$ and $m_1^{(A1)} = m_1^{(A3)} = 5$ Kg, the relationship between t_{A1} and t_{A3} turns into $t_{A1} = \left(a_1^{(A1)}/a_1^{(A3)}\right)t_{A3}$. It is also noted that $\dot{\theta}_1^{(A1)}(t_{A1}) = \dot{\theta}_1^{(A3)}(t_{A3})\sqrt{G^{(A1)}/G^{(A3)}}$. Using the same manipulations, it yields that $\dot{\theta}_1^{(A1)}(t_{A1}) = \left(a_1^{(A3)}/a_1^{(A1)}\right)\dot{\theta}_1^{(A3)}(t_{A3})$. The similar procedure is able to find the solution for $\theta_2(t)$.

According to the above results, the following findings at impact are observed for golfers A1 and A3 when the same ratio of club length to arm length k_1 is applied (t_{imp} denotes impact time).

$$\dot{\theta}_1^{(A1)}\left(t_{imp}^{(A1)}\right) = \left(a_1^{(A3)}/a_1^{(A1)}\right)\dot{\theta}_1^{(A3)}\left(t_{imp}^{(A3)}\right) \tag{4-5}$$

$$\dot{\theta}_2^{(A1)}\left(t_{imp}^{(A1)}\right) = \left(a_1^{(A3)}/a_1^{(A1)}\right)\dot{\theta}_2^{(A3)}\left(t_{imp}^{(A3)}\right) \tag{4-6}$$

$$\theta_1^{(A1)}\left(t_{imp}^{(A1)}\right) = \theta_1^{(A3)}\left(t_{imp}^{(A3)}\right) \tag{4-7}$$

$$\theta_2^{(A1)}\left(t_{imp}^{(A1)}\right) = \theta_2^{(A3)}\left(t_{imp}^{(A3)}\right) \tag{4-8}$$

$$t_{imp}^{(A1)} = \left(a_1^{(A1)}/a_1^{(A3)}\right)t_{imp}^{(A3)} \tag{4-9}$$

The equations of the horizontal club head speed v_h at impact for A1 and A3 are expressed as

$$v_h^{(A1)} = -a_1^{(A1)}\dot{\theta}_1^{(A1)}\left(t_{imp}^{(A1)}\right)Sin\left(\theta_1^{(A1)}\left(t_{imp}^{(A1)}\right)\right) - a_2^{(A1)}\left(\dot{\theta}_1^{(A1)}\left(t_{imp}^{(A1)}\right)+\dot{\theta}_2^{(A1)}\left(t_{imp}^{(A1)}\right)\right)Sin\left(\theta_1^{(A1)}\left(t_{imp}^{(A1)}\right)+\theta_2^{(A1)}\left(t_{imp}^{(A1)}\right)\right) \tag{4-10}$$

and

$$v_h^{(A3)} = -a_1^{(A3)}\dot{\theta}_1^{(A3)}\left(t_{imp}^{(A3)}\right)Sin\left(\theta_1^{(A3)}\left(t_{imp}^{(A3)}\right)\right) - a_2^{(A3)}\left(\dot{\theta}_1^{(A3)}\left(t_{imp}^{(A3)}\right)+\dot{\theta}_2^{(A3)}\left(t_{imp}^{(A3)}\right)\right)Sin\left(\theta_1^{(A3)}\left(t_{imp}^{(A3)}\right)+\theta_2^{(A3)}\left(t_{imp}^{(A3)}\right)\right) \tag{4-11}$$

Substituting Eq. (4-5)-(4-8) into Eq. (4-10) and considering $a_1^{(A3)}/a_1^{(A1)} = a_2^{(A3)}/a_2^{(A1)}$, it yields

$$v_h^{(A1)} = v_h^{(A3)} \tag{4-12}$$

We also assume that there are a group B comprising three golfers named B1, B2 and B3 with the same arm length 0.60 m but different masses 5 Kg, 6 Kg and 7Kg respectively, and they play the same length 1.11 m and equivalent k_2 golf clubs. The reasoning is carried out just as that for group A on condition of $k_1 = 1.85$ and $k_2^{(B1)} = k_2^{(B3)}$. The results are shown below:

$$\dot{\theta}_1^{(B1)}\left(t_{imp}^{(B1)}\right) = \sqrt{m_1^{(B3)}/m_1^{(B1)}}\,\dot{\theta}_1^{(B3)}\left(t_{imp}^{(B3)}\right) \tag{4-13}$$

$$\dot{\theta}_2^{(B1)}\left(t_{imp}^{(B1)}\right) = \sqrt{m_1^{(B3)}/m_1^{(B1)}}\,\dot{\theta}_2^{(B3)}\left(t_{imp}^{(B3)}\right) \tag{4-14}$$

$$\theta_1^{(B1)}\left(t_{imp}^{(B1)}\right) = \theta_1^{(B3)}\left(t_{imp}^{(B3)}\right) \tag{4-15}$$

$$\theta_2^{(B1)}\left(t_{imp}^{(B1)}\right) = \theta_2^{(B3)}\left(t_{imp}^{(B3)}\right) \tag{4-16}$$

$$t_{imp}^{(B1)} = \sqrt{m_1^{(B1)}/m_1^{(B3)}}\,t_{imp}^{(B3)} \tag{4-17}$$

Similarly, Substituting Eq. (4-13)-(4-16) into the expression of the horizontal club head speed at impact, which is the same one as Eq. (4-10), we obtain

$$v_h^{(B1)}\left(t_{imp}^{(B1)}\right) = \sqrt{m_1^{(B3)}/m_1^{(B1)}}\,v_h^{(B3)}\left(t_{imp}^{(B3)}\right) \tag{4-18}$$

Although only two of the three golfers in group A and B are studied, it is no doubt that the results are also verifiable to any two of them.

Numerical simulation is carried out for group A and B in order to explicitly indicate the influence of the interactions on the downswing. The simulation results indicate that different mass or length ratios of clubs to arms lead to various impact time (Figure 4-1 and Figure 4-2). For group A and B, the larger the mass or length ratio of clubs to arms, the larger the impact time is. This means that the impact time will become large when the mass or length of golf club is increased. The golf club position at impact is defined in Figure 4-3. As we can see from Figure 4-4 and Figure 4-5, the same golf club position is exhibited at impact when the mass or length ratios of clubs to arms are equal. This point can be used to explain the phenomenon that different-arm golfers are able to obtain the almost same golf club position at impact even if they hold different golf clubs during the golf-playing. Figure 4-6 shows that the horizontal club head speeds at impact for the three members in group A are equal with the same length ratio of clubs to arms, even if their arm lengths are different. The horizontal club head speed at impact is shown to be enhanced for every golfer with the increase of the length ratio. This means that the lengthening of the golf club effectively increases the horizontal club head speed at impact [21]. Figure 4-7 indicates that the same mass ratio of clubs to arms results in different club head speed at impact. So it is clear that the arm and club masses are two important factors to determine the final club head speed at impact. This point can be confirmed by Figure 4-8 and Figure 4-9.

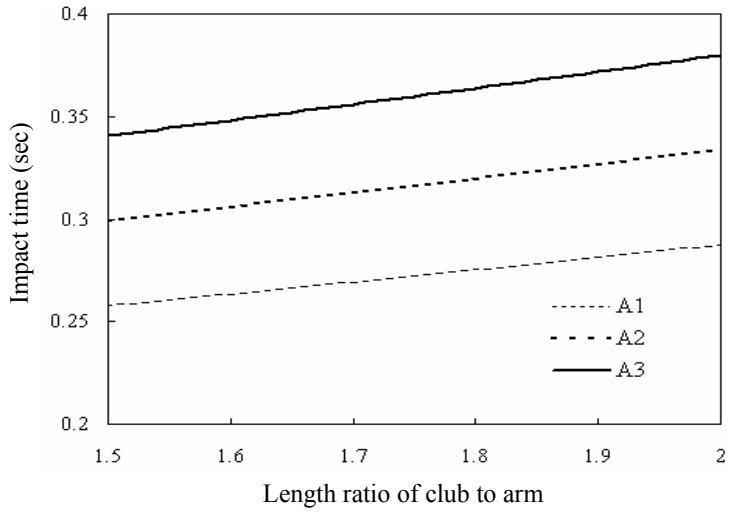

Figure 4-1 Impact time when different length ratios of clubs to arms are applied.

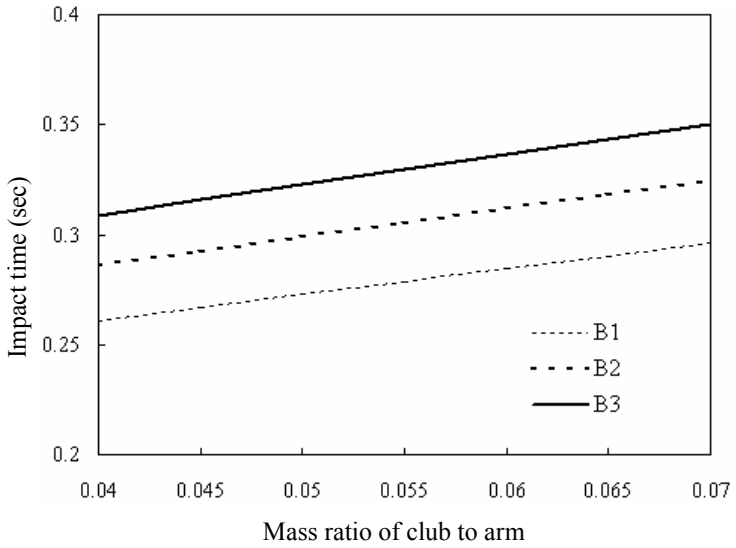

Figure 4-2 Impact time when different mass ratios of clubs to arms are applied

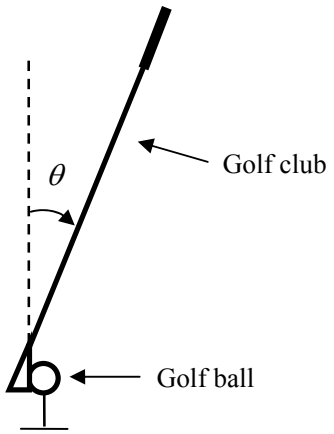

Figure 4-3 Golf club position, θ, at impact for a right-handed golfer when viewed 'face-on'.

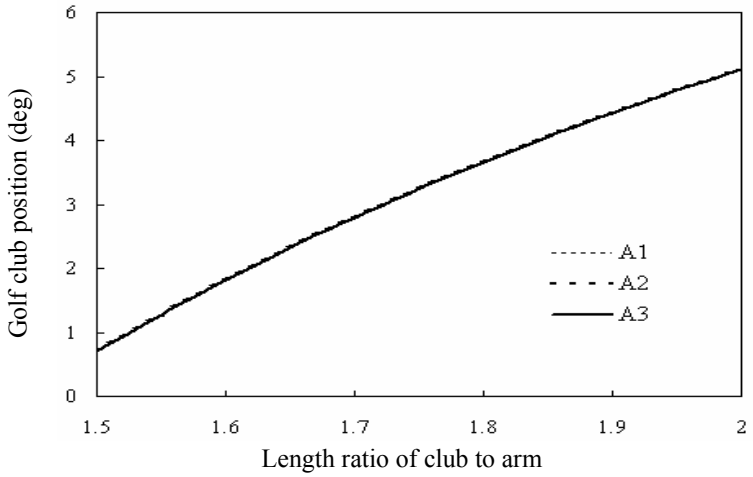

Figure 4-4 Golf club position when different length ratios of clubs to arms are applied

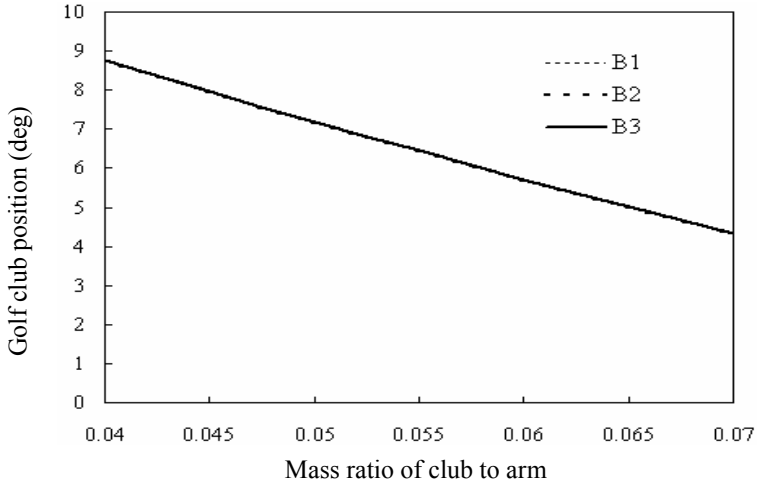

Figure 4-5 Golf club position when different mass ratios of clubs to arms are applied

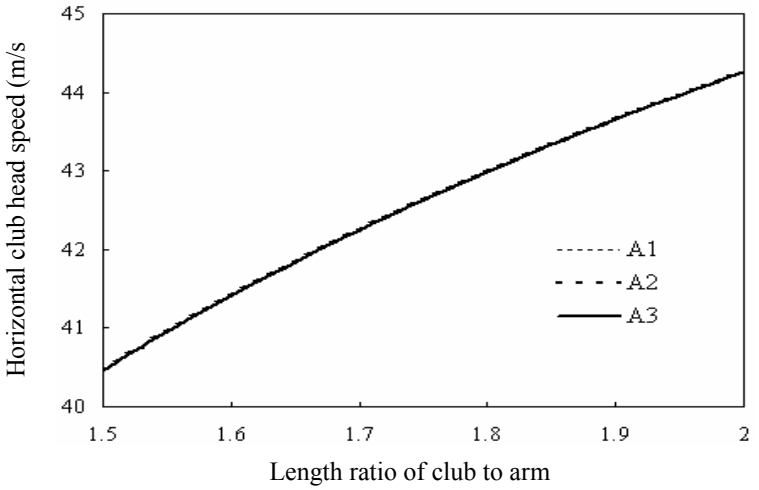

Figure 4-6 Horizontal club head speed at impact when different length ratios of clubs to arms are applied

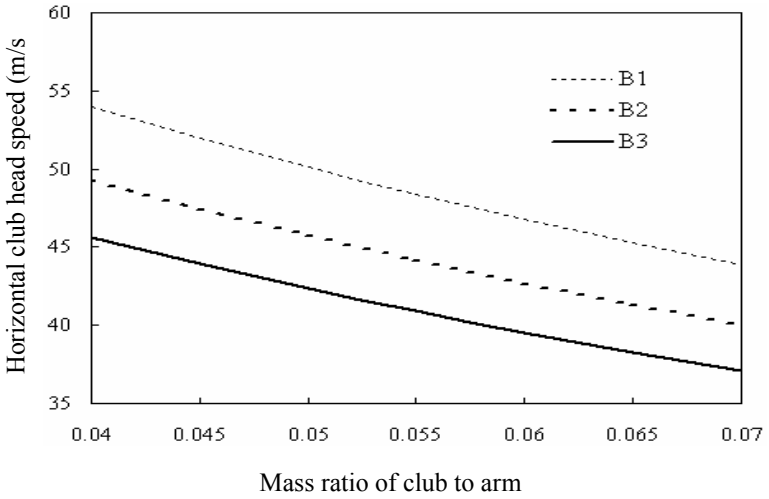

Figure 4-7 Horizontal club head speed at impact when different mass ratios of clubs to arms are applied

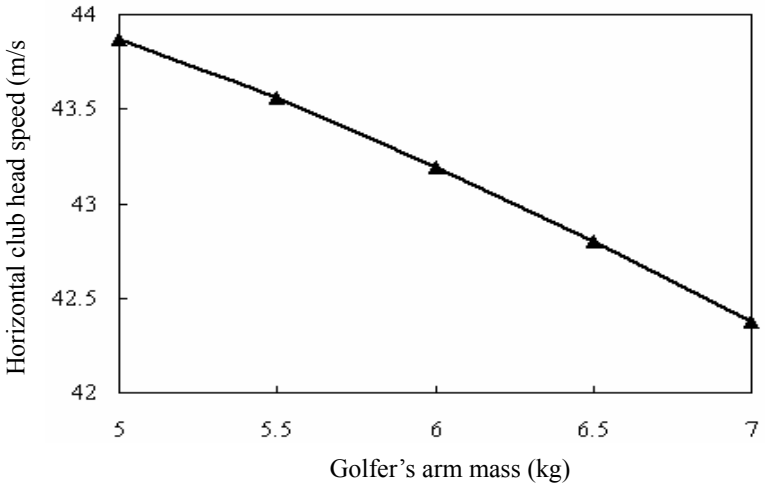

Figure 4-8 Horizontal club head speed at impact when golfers, with the same arm length 0.6 m but different masses, play a golf club of 0.35 kg in mass and 1.10 m in length;

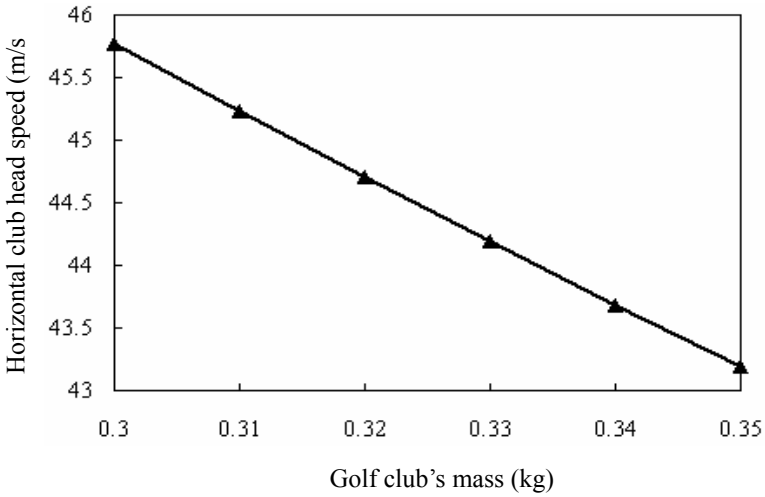

Figure 4-9 Horizontal club head speed at impact when a golfer, with an arm of 6 kg in mass and 0.6 m in length, play golf clubs with the same length 1.10 m but different masses.

4.3 Summary

The aim of this chapter is to gain an understanding of the interactions between golfer's arms and golf clubs in the golf downswing. A 2-dimensional double pendulum model of the golf swing with the normalized parameters is used to analyze how the interactions influence the golf swing. The results show that the length and, in particular the mass ratios of clubs to arms are important parameters which eventually affect impact time, the horizontal club head speed and club positions at impact. Numerical simulation is carried out to describe the effects of these ratios upon the golf swing.

Chapter 5

Impedance control for a prototype of golf swing robot

5.1 Mathematical model

In order to demonstrate the validity of the impedance control method, the swing motions of different-arm-mass golfers should be obtained so that the motions can be compared with those from the proposed golf swing robot using the impedance control method. Therefore, a dynamic model developed in Chapter 3 is used to emulate the swing motions of different-arm-mass golfers under a given input torque of the shoulder joint. It should be noticed that the impedance of the wrist joint (wrist action) is also considered in this model. The wrist impedance function can be simply written as

$$\tau_f = c\dot{\beta} \tag{5-1}$$

Where c is the viscous damping constant of the wrist joint; τ_f is the wrist retarding torque due to the impedance of the wrist joint.

Since professional golfers such as legendary Bobby Jones [22] turned the wrist joint freely and felt that the golf club freewheeled at the latter stage of the downswing, the value of c used here is relatively small as compared to that from Milne and Davis [7]. Here, it is assumed that the value of c is equivalent to that of the golf swing robot. So the equations of motion of golf swing are given by.

$$\boldsymbol{B}(\boldsymbol{\theta})\ddot{\boldsymbol{\theta}}+\boldsymbol{h}(\boldsymbol{\theta},\dot{\boldsymbol{\theta}})+\boldsymbol{K}\boldsymbol{\theta}+\boldsymbol{G}(\boldsymbol{\theta})+\boldsymbol{D}\dot{\boldsymbol{\theta}}=\boldsymbol{\tau} \tag{5-2}$$

Where

$$\boldsymbol{B}=\begin{bmatrix} B_{11} & B_{12} & B_{13} & B_{14} \\ B_{21} & B_{22} & B_{23} & B_{24} \\ B_{31} & B_{32} & B_{33} & B_{34} \\ B_{41} & B_{42} & B_{43} & B_{44} \end{bmatrix}, \boldsymbol{\theta}=\begin{bmatrix} \alpha \\ \beta \\ q_1 \\ q_2 \end{bmatrix}, \boldsymbol{h}=\begin{bmatrix} h_1 \\ h_2 \\ h_3 \\ h_4 \end{bmatrix}, \boldsymbol{K}=\begin{bmatrix} 0 & 0 & 0 & 0 \\ 0 & 0 & 0 & 0 \\ 0 & 0 & K_{33} & K_{34} \\ 0 & 0 & K_{34} & K_{44} \end{bmatrix}$$

$$\boldsymbol{G}=\begin{bmatrix} G_1 \\ G_2 \\ G_3 \\ G_4 \end{bmatrix}, \boldsymbol{D}=\begin{bmatrix} 0 & 0 & 0 & 0 \\ 0 & c & 0 & 0 \\ 0 & 0 & d_1 & 0 \\ 0 & 0 & 0 & d_2 \end{bmatrix}, \boldsymbol{\tau}=\begin{bmatrix} \tau_1 \\ \tau_2 \\ 0 \\ 0 \end{bmatrix}$$

c is the wrist viscosity coefficient.

5.2 Impedance control design

The dynamic equation of a mechanical system is always expressed as

$$\boldsymbol{M}\,\ddot{\boldsymbol{x}}+\boldsymbol{C}\,\dot{\boldsymbol{x}}+\boldsymbol{K}\,\boldsymbol{x}=\boldsymbol{F} \tag{5-3}$$

Where $\boldsymbol{F}$ is the external force; $\boldsymbol{M}$, $\boldsymbol{C}$ and $\boldsymbol{K}$ are denoted as the inertia, viscosity and stiffness, respectively. These parameters are called as mechanical impedance in the work of Hogan [23]. In this study, a golfer's arm as a mechanical system is investigated. Since it has been found that a golfer's hands move in a circular arc about the shoulder joint during the golf swing, the golfer's arm is assumed to be a rigid body and the stretch reflex of the arm muscle is neglected. The fact that the swing motions obtained from the numerical simulation using the rigid arm link agree well with those from the swing photographs of professional golfers have assured the above assumption [1-7]. Therefore, the dynamic equation of the golfer's arm can be given by

$$\boldsymbol{M}\,\ddot{\boldsymbol{x}}=\boldsymbol{F} \tag{5-4}$$

Where the viscosity and stiff of the golfer's arm is neglected and the moment of

inertia of the arm about the shoulder joint, ***M***, is defined as the mechanical impedance. The virtual system representing the dynamic model of a golfer's arm and the robot system expressing the dynamic model of a robot's arm are shown in Figure 5-1 and Figure 5-2, respectively.

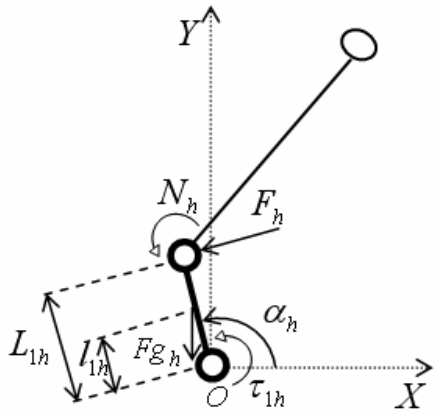

Figure 5-1 Virtual system

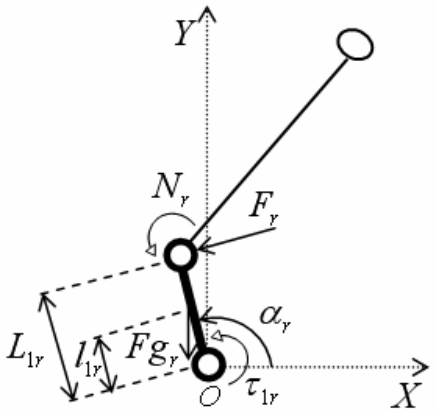

Figure 5-2 Robot system

The equations of motion of the virtual and robot systems are written as Eq. (5-5) and Eq. (5-6).

$$J_{1h}\ \ddot{\alpha}_h = \tau_{1h} + F_h\ L_{1h} + fg_h(\alpha_h) + N_h \tag{5-5}$$

$$J_{1r}\ \ddot{\alpha}_r = \tau_{1r} + F_r\ L_{1r} + fg_r(\alpha_r) + N_r \tag{5-6}$$

Where the subscripts *h* and *r* denote the golfer and robot, respectively; $fg(\alpha) = -Fg\, l_1 \cos\alpha$; *Fg* is the gravitational force of the arm; *F* is the reaction force from the club to arm, and the direction is perpendicular to the arm; *N* is the reaction torque from the club to arm; Here, we assume $L_{1h} = L_{1r}$.

In our control method, the dynamic parameters J_{1h} and J_{1r} in Eq. (5-5) and Eq. (5-6) are defined as the mechanical impedance. With the various arm masses for the golfer and robot, the mechanical impedance J_{1h} and J_{1r} are varied. As a result, the swing motion of the robot is not the same as that of the golfer, even if the input torques of the shoulder

joints are equal. In order to realize the dynamic swing motion of the virtual system, the following control algorithm is proposed for the robot.

According to the Euler method, angular acceleration of the arm can approximate to the following expressions.

$$\ddot{\alpha}_h^n = \frac{\dot{\alpha}_h^n - \dot{\alpha}_h^{n-1}}{\Delta t}, n = 1, \ldots M. \tag{5-7}$$

$$\ddot{\alpha}_r^n = \frac{\dot{\alpha}_r^n - \dot{\alpha}_r^{n-1}}{\Delta t}, n = 1, \ldots M. \tag{5-8}$$

Where Δt is the sampling time; M is an integer; $\dot{\alpha}^n, \ddot{\alpha}^n$ are the angular velocity and acceleration in the *nth* sampling period.

Substituting Eq. (5-7) into Eq. (5-5), and Eq. (5-8) into Eq. (5-6), and after some manipulations, Eq. (5-9) and Eq. (5-10) are obtained.

$$\dot{\alpha}_h^n = \dot{\alpha}_h^{n-1} + \frac{\Delta t}{J_{1h}}\left(\tau_{1h}^{n-1} + F_h^{n-1} L_{1h} + fg_h\left(\alpha_h^{n-1}\right) + N_h^{n-1}\right) \tag{5-9}$$

$$\dot{\alpha}_r^n = \dot{\alpha}_r^{n-1} + \frac{\Delta t}{J_{1r}}\left(\tau_{1r}^{n-1} + F_r^{n-1} L_{1r} + fg_r\left(\alpha_r^{n-1}\right) + N_r^{n-1}\right) \tag{5-10}$$

In the impedance control method, the arm angular velocity of the golfer is regarded as the control input reference for the robot. As shown in Eq. (5-9), the reaction force F_h^{n-1} and reaction torque N_h^{n-1} should be known in advance, if we expect to acquire the control input reference $\dot{\alpha}_h^n$. Since the PI control in the velocity loop for the robot is used to assure that the arm angular velocity of the robot is equivalent to that of the golfer, $\dot{\alpha}_h = \dot{\alpha}_r$, the motions of the same golf club used by the golfer and robot are the same. Therefore, the reaction force and reaction torque from the same golf club to the arms of the golfer and robot are equal, that is, $F_h^{n-1} = F_r^{n-1}$ and $N_h^{n-1} = N_r^{n-1}$. Note that the

reaction force F_r^{n-1} and reaction torque N_r^{n-1} can be obtained by a 6-dimensional force sensor and a 1-dimensional force sensor installed on the robot's arm, respectively. Substituting the above results into Eq. (5-9), the control input reference $\dot{\alpha}_h^n$ for the golf swing robot can be calculated from the following equation.

$$\dot{\alpha}_h^n = \dot{\alpha}_h^{n-1} + \frac{\Delta t}{J_{1h}}\left(\tau_{1h}^{n-1} + F_r^{n-1} L_{1h} + fg_h\left(\alpha_r^{n-1}\right) + N_r^{n-1}\right) \tag{5-10}$$

where the input torque of the shoulder joint for a golfer τ_{1h}^{n-1} can be given by the operator of the robot.

The whole configuration of the control system is described as Figure 5-3.

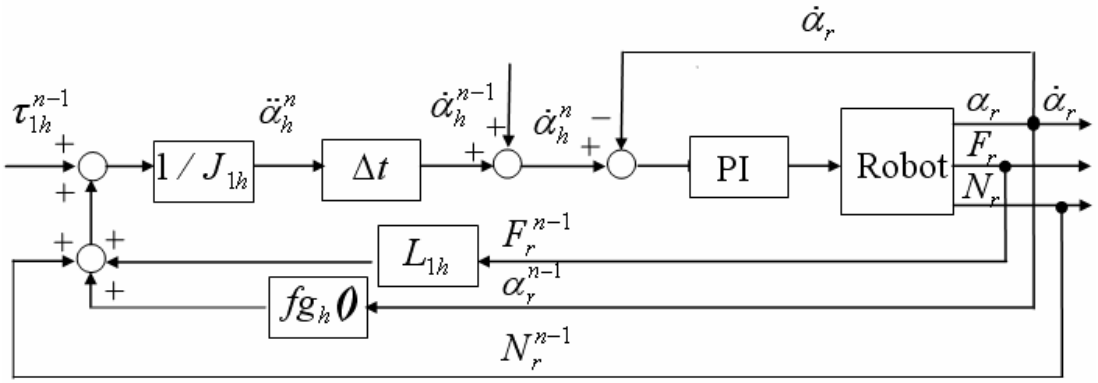

Figure 5-3 Configuration of the control system

5.3 Simulation

A fourth-order-Runge-Kutta integration method at intervals of 1.0×10^{-4} s was used to drive the golfer swing model and the swing motions of different-arm-mass golfers were obtained.

5.4 Experiment

The experiment was implemented by a prototype of golf swing robot composed of

an actuated joint driven by a direct drive motor (NSK MEGATORQUE) and a passive joint with a mechanical stopper. The stopper carries out the wrist cock action. A mechanical brake is used to stop the golf club after impact. An absolute resolver (feedback signal 51200 pulse/rev) and an incremental encoder (9000 pulse/rev) situated at the actuated and passive joints are utilized to measure the arm and club rotational angles, respectively. A 1-dimensional force sensor (KYOWA LCN-A-500N) and a 6-dimensional force sensor (NITTA IFS-67M25A50-I40) are adopted to obtain the reaction torque N_r and reaction force F_r from the club to arm, respectively. A flexible solid beam made of aluminium is used to replace the shaft, and it is clamped at the grip. The natural frequencies and vibration mode shapes of the golf club are obtained by numerical calculation and experimental modal analysis. The configuration of the experiment modal analysis system for the golf club is shown in Figure 5-4. Figure 5-5 shows the first and second mode shapes of the golf club used in our simulation (MAM), and those obtained from experimental modal analysis (EMA). It is evident that the mode shapes of the golf club applied in our simulation are consistent well with those obtained form experimental modal analysis.

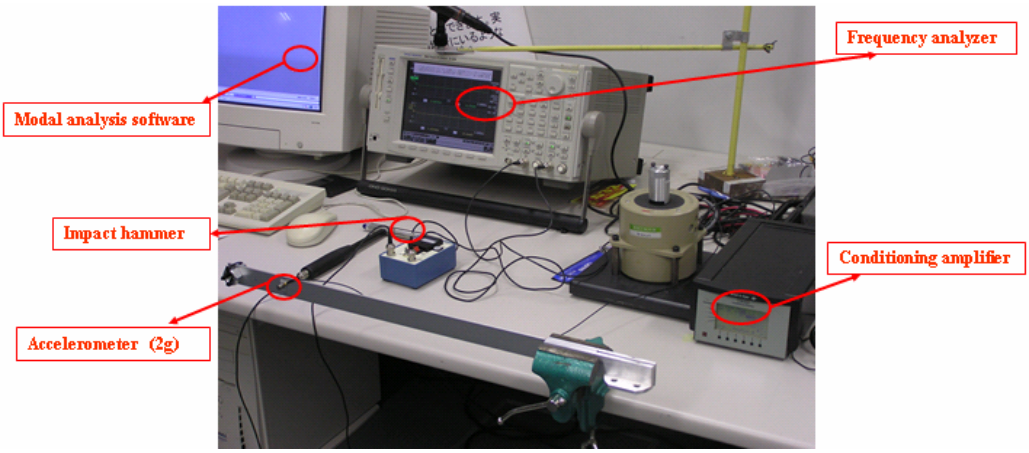

Figure 5-4 Configuration of the modal analysis system

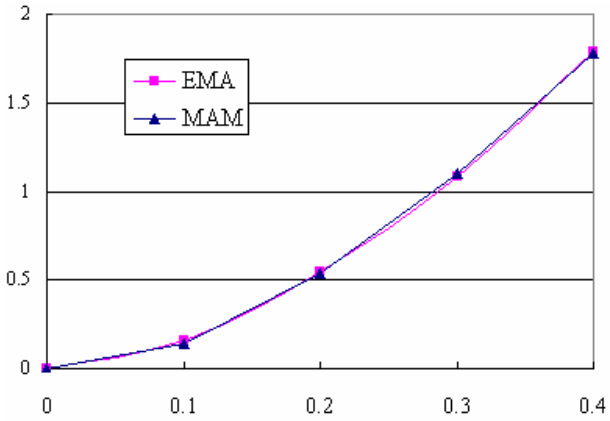

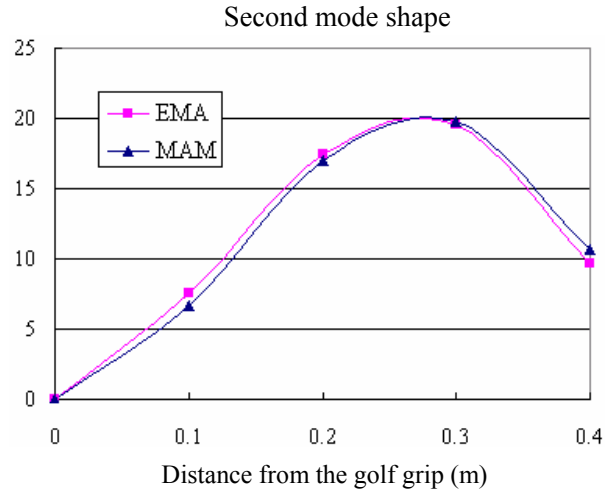

Figure 5-5 Comparison of the mode shapes of the golf club, which used in our simulation (MAM) or obtained from experimental modal analysis (EMA)

The photograph of the robot system is shown in Figure 5-6. Table 5-1 gives the parameters of the robot system. The experimental control system is indicated schematically in Figure 5-7. A personal computer is used to implement the impedance control program and its sampling rate is 1KHz. By using the velocity control mode of the motor driver, the DD motor is controlled by the velocity (voltage) reference from a D/A converter (CONTEC, DA12-16(PCI)). Here, JR3 is a DSP-based signal receiver for the 6-dimensional force sensor.

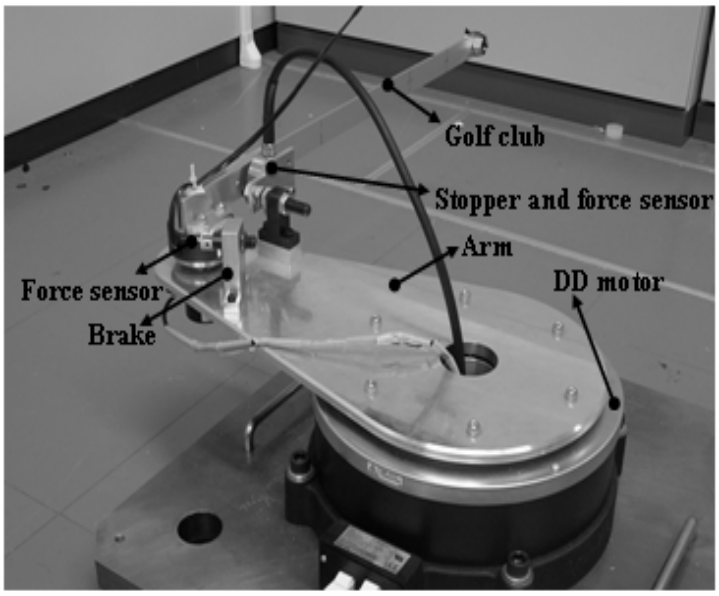

Figure 5-6 Prototype of golf swing robot

Table 5-1 Parameters of the robot system

Parameter	Symbol	Value
Mass of arm	m_1	3.779 kg
Moment of inertia of arm about shoulder joint O	J_1	0.082 kg m^2
Length of arm	a_1	0.3 m
Mass of hand-grip	m_2	0.603 kg
Moment of inertia of hand-grip	J_2	6.40×10^{-4} kg m^2
Length of hand-grip	a_2	0.108 m
Mass per unit length of shaft	ρ	0.242 kg/m
Length of shaft	a_3	0.5 m
Area moment of inertia of shaft	I	6.75×10^{-11} m^4
Young's modulus of shaft material	E	7.00×10^{10} N/m^2
Mass of club head	m_R	0.06 kg
Moment of inertia of club head	J_R	6.89×10^{-6} kg m^2
Radius of club head	R	0.007 m
Wrist viscous damping coefficient	c	0.033 N m s/rad
Damping coefficient of first mode of club	d_1	0.269 N s/m
Damping coefficient of second mode of club	d_2	0.490 N s/m

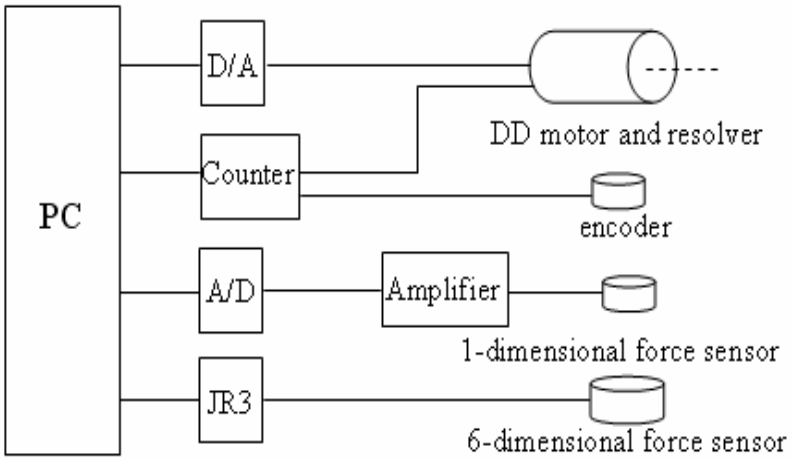

Figure 5-7 Schematic diagram of the experimental control system

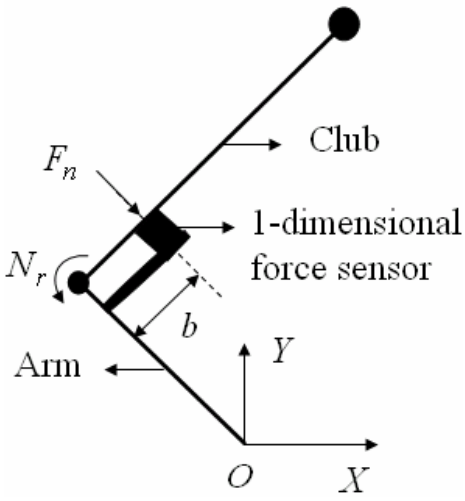

Figure 5-8 Obtainment of the reaction torque N_r

The obtainment of the reaction torque N_r is shown in Figure 5-8. Based on the figure, the reaction torque N_r can be calculated by

$$N_r = -F_n\, b \tag{5-11}$$

where F_n is the force measured from the 1-dimensional force sensor; b is the distance between the force contact point of the sensor and the wrist joint of the robot.

It is noted that not only the force measured from the 6-dimensional force sensor is needed to calculate the reaction force F_r, but also the inertia force of the sensor f_t caused by the arm angular acceleration $\ddot{\alpha}_r$ should be considered because the sensor is regarded as a part of hand-grip. The specific force analysis of the hand-grip is shown in Figure 5-9.

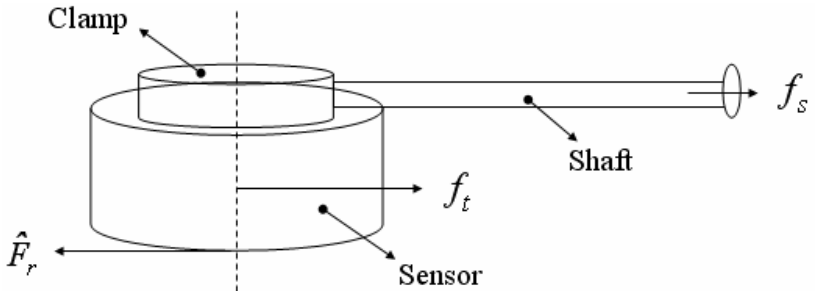

Figure 5-9 Force analysis of the hand-grip

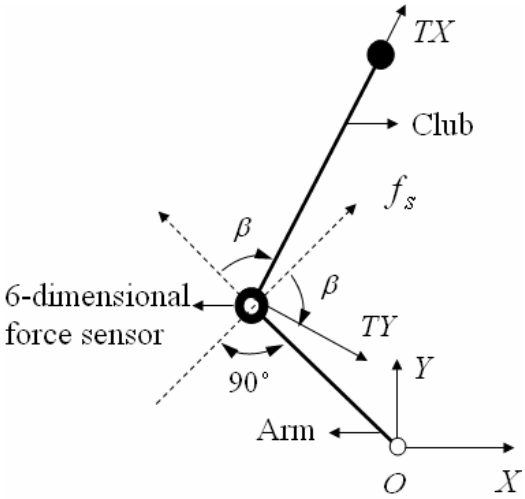

Figure 5-10 Obtainment of the force f_s whose direction is perpendicular to the arm

According to the figure 5-9, the following equations are obtained.

$$\hat{F}_r = f_t + f_s \tag{5-12}$$

$$f_t = m_s \ddot{\alpha}_r L_{1r} \tag{5-13}$$

$$F_r = -\hat{F}_r \tag{5-14}$$

where m_s is the sensor mass; $\hat{F}_r$ is the reaction force from the arm to club; f_s is the force

obtained from the sensor, and its direction is perpendicular to the arm, as shown in Figure 5-10. The force f_s can be calculated by

$$f_s = -TX\ \boldsymbol{sin}(\beta) + TY\ \boldsymbol{cos}(\beta) \tag{5-15}$$

where TX and TY are the forces measured from the 6-dimensional force sensor, and they are perpendicular with each other.

Therefore, the reaction force F_r from the club to arm is obtained as

$$F_r = -m_s\ \ddot{\alpha}_r\ L_{1r} + TX\ \boldsymbol{sin}(\beta) - TY\ \boldsymbol{cos}(\beta) \tag{5-16}$$

In Eq. (5-16), the arm angular acceleration $\ddot{\alpha}_r$ should be known in order to calculate the reaction force F_r. Here, a constant-coefficient kalman filter is used to obtain the arm angular velocity to reject undesirable position measurement noise, and then $\ddot{\alpha}_r$ is acquired by the filtered velocity using the difference method.

Lampsa [14] thought that a pause usually occurs at the moment when a golfer completes his backswing and is just about to begin his downswing, indicating that the angular velocities of the arm and club are equal to zero at the start of the downswing. Therefore, it is assumed in this study that the swing commences with $\dot{\alpha} = 0, \dot{\beta} = 0$ and the bending of the golf shaft at the start of the downswing is also ignored. The posture values of the arm and club at the start of the downswing are taken with $\alpha = 120^\circ, \beta = -90^\circ$, which were regarded as the general initial configuration for professional golfers in the work of Sprigings [9]. The simulation and experiment are terminated when the club head hits the golf ball, and the ball is placed at the center of the width of the golfer's stance (the same golf ball position is shown in Figure 7-8 in Jorgensen [3]).The gravity effect is neglected because of the horizontal positioning of the direct drive motor. The golf swing robot is defined as R, and three golfers, labelled

by H1, H2 and H3, own the same arm length as that of the robot but with different arm masses, 5kg, 3kg and 2kg, respectively. It has been noted that there are many kinds of torque input functions of the shoulder joint applied in the previous research work of golf swing, and here these functions are referred to as τ_1 employed at the shoulder joint *O*. Jorgensen [1] thought that the shoulder input torque was constant during the swing, Milne and Davis [7] used a ramp as the torque function and Suzuki and Inooka [12] set the torque function as a trapezoid. In the present study, a trapezoid-shaped torque (Figure 5-11) is employed at the shoulder joint for the golfers. The torque is linearly increased with the rise time 0.148s and then up to the maximum amplitude 10 Nm which is maintained 0.05s, and finally is terminated at the time of 0.346s. By this torque, the suitable postures of the arm and club at impact for the general golfers with 5kg arm can be obtained: the arm and club will be a vertical line at impact, that is, $\alpha = 270^\circ$, $\beta = 0^\circ$.

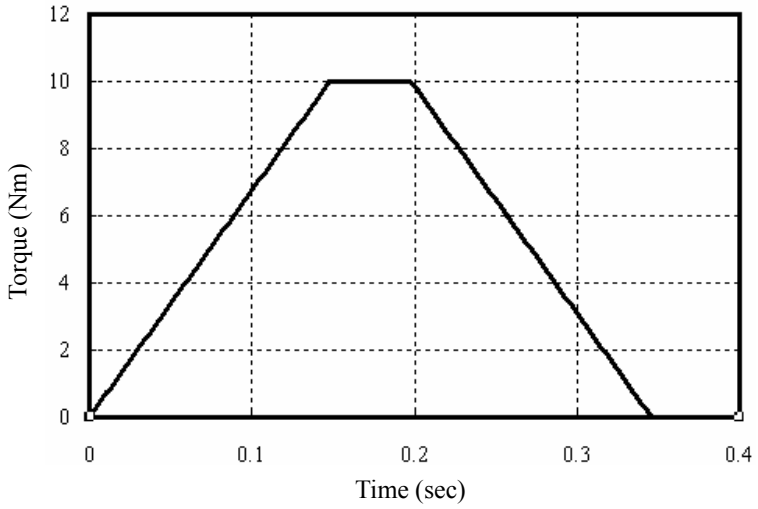

Figure 5-11 Torque of shoulder joint

5.5 Results and discussion

Figure 5-12 shows the results of a comparison of the arm and club rotational angles

for the robot and different-arm-mass golfers. It is observed that the swing trajectories of the arm (Figure 5-12 (a), (c), (e)) and club (Figure 5-12 (b), (d), (f)) for H1, H2 and H3 are not the same. The comparison of the arm and club angular velocities for the robot and different-arm-mass golfers is shown in Figure 5-13. It can be seen that the angular velocities of the arm (Figure 5-13 (a), (c), (e)) and club (Figure 5-13 (b), (d), (f)) are also different for three golfers. The maximum arm angular velocity of H3 is obviously larger than those of H1 and H2, and the increases are 2.86 rad/s and 1.16 rad/s as compared to H1 and H2, respectively. It is also clear that the club angular velocities are different for them and the maximum club angular velocity of H3 is larger than those of H1 and H2, and the increases are 5.16 rad/s and 2.30 rad/s, respectively. From Figure 5-12 (a), (c), (e) and Figure 5-13 (a), (c), (e), it can be seen that the swing motions of the arm of the proposed golf swing robot agree well with those of the three golfers. As for the swing motions of the club, it shows that no substantial differences are found between the robot and golfers in Figure 5-12 (b), (d), (f) and Figure 5-13 (b), (d), (f). However, it is noteworthy to mention that the club swing motion differences between the robot and golfers will become large with the higher club angular velocity (For example, see Figure 5-12 (b), (f)). This can be explained from the fact that the higher club angular velocity causes a larger air drag force which retards the club in the swing experiment for the robot, and this retarding force, however, is neglected in the simulation of the swing motion for the golfer due to the complex dynamical modelling and practical measurement difficulty for this air drag force.

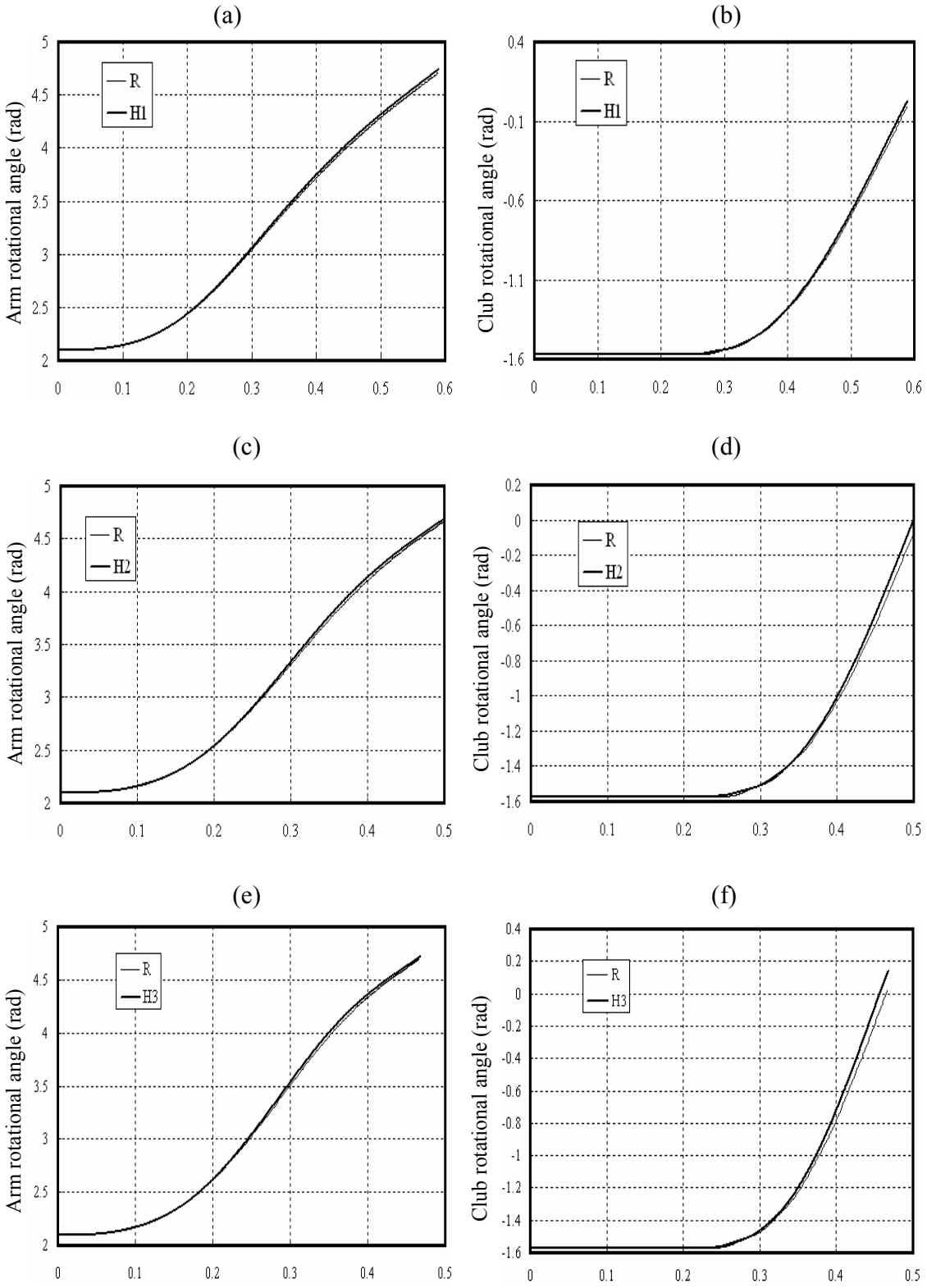

Figure 5-12 Comparison of arm and club rotational angles for the robot and different-arm-mass golfers

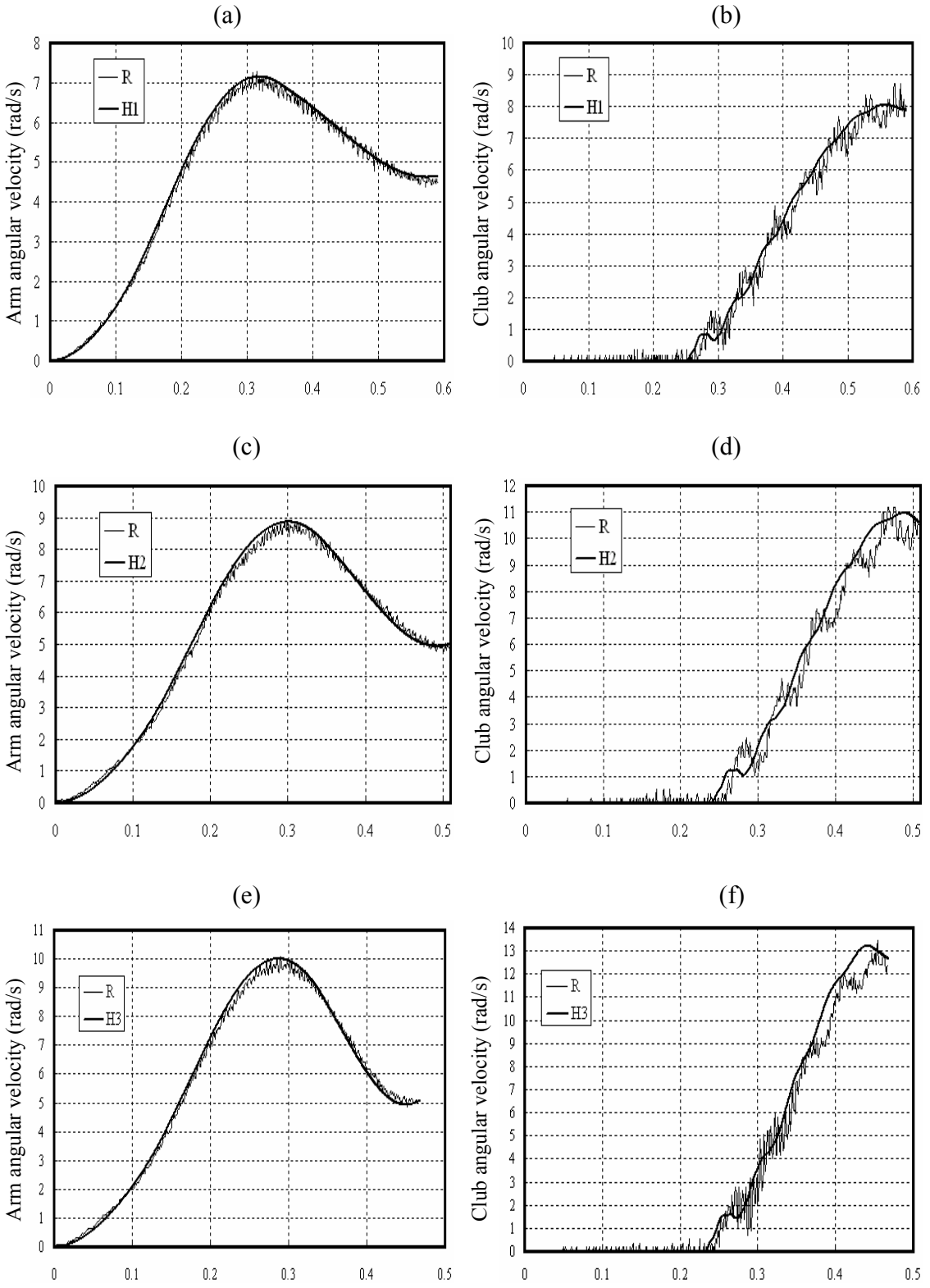

Figure 5-13 Comparison of arm and club angular velocities for the robot and different-arm-mass golfers

Through the above comparisons, it is shown that the swing motions of different-arm-mass golfers are not the same even if the shoulder input torques used by them are equivalent and the proposed golf swing robot using the impedance control method can emulate the swing motions of different-arm-mass golfers.

We should note that in our control method the control reference for the robot - arm angular velocity of a golfer is determined by the feedback signals such as the reaction force and torque from the club to the arm. Since the arm angular acceleration is approximated by the Euler method, the control reference in the nth sampling period is calculated by the feedback signals in the (n-1)th sampling period (Eq. (5-10)). Therefore, a sampling period time-delay error occurs. In order to solve this problem, we would have to adopt the relatively small sampling control period to limit the control error. In this study, the 1ms sampling control period was used and the satisfying results were achieved (Figure 5-12 and Figure 5-13). We are also expected to investigate whether a longer sampling control period such as 4 ms and 10 ms would lead to some good experiment results as compared to 1ms.

Figure 5-14 shows the results of a comparison of the arm and club angular velocities for the robot and different-arm-mass golfers while using the 4ms sampling control period. We note that the swing motions of different-arm-mass golfers still can be emulated by the robot with the 4ms sampling control period. But it is clear that the 10 ms sampling control period can not give the satisfying experiment results, in particular when the swing speed of the robot is increasingly high (Figure 5-15 (c) and Figure 5-15 (d)).

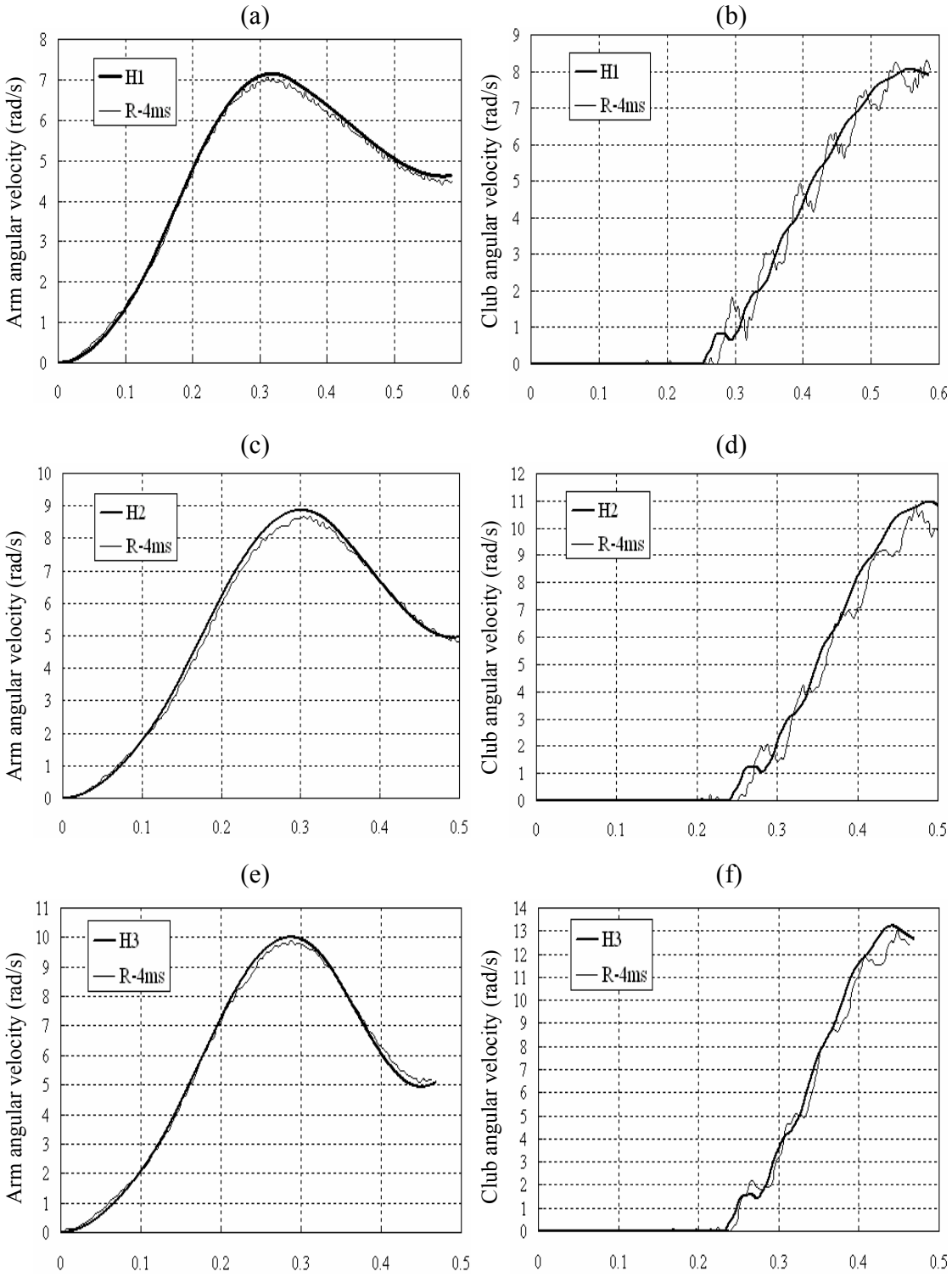

Figure 5-14 Comparison of arm and club angular velocities for the robot and different-arm-mass golfers using the 4ms sampling control period

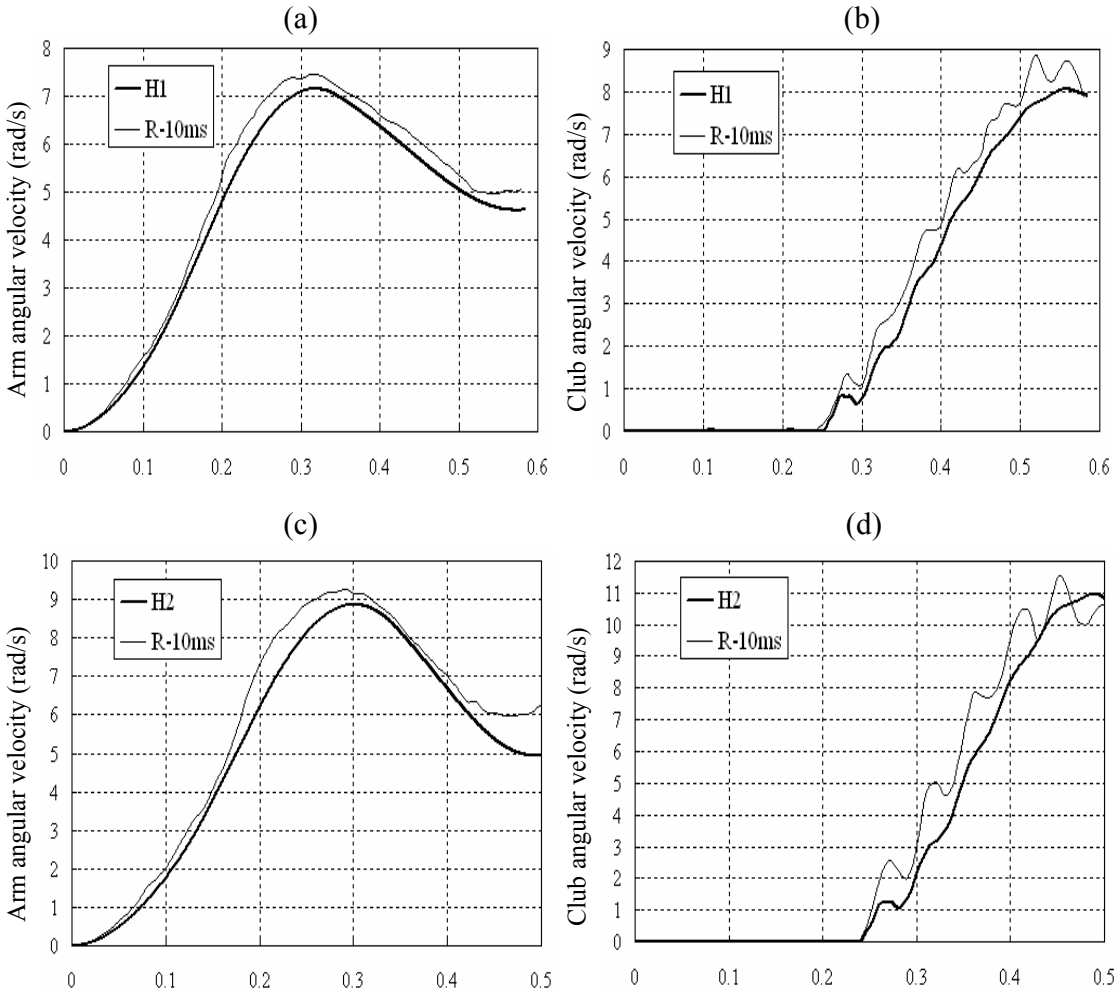

Figure 5-15 Comparison of arm and club angular velocities for the robot and different-arm-mass golfers using the 10 ms sampling control period

5.6 Summary

Various golfers can play different golf swing motions even though they use the same golf club. This phenomenon casts light on the significance of the dynamic interactions between a golfer's arms and a golf club. Unfortunately, the influence of the dynamic interactions were not considered in the conventional control of a golf swing robot, though such interaction does result in different swing motions, even though the robot has the same input torque of the shoulder joint as the golfer's. An impedance control method is thus proposed for a prototype of golf swing robot to emulate the swing motions of the different-arm-mass golfers in consideration of the dynamic interactions between arms and golf clubs. Based on the Euler-Lagrange principle and assumed modes technique, a mathematical model of golf swing, considering the bending flexibility and centrifugal stiffening of the golf shaft, is established to simulate the swing motions of different-arm-mass golfers. The impedance control method is implemented to a prototype of golf swing robot composed of one actuated joint and one passive joint. The comparison of the swing motions between the robot and different-arm-mass golfers is made and the results show that the proposed golf swing robot with the impedance control method can emulate the swing motions of the different-arm-mass golfers.

Chapter 6

Conclusions

A golf stroke by an accomplished golfer is usually a thing of beauty. There are a large number of books on golf, most of them are written by golfers who have owned the perfect skills of golf swing. These works are mainly concerned with the swing skill instructions that leave the reader with little understanding of what actually happens during a golf swing. Therefore, the mathematical modelling of the golf swing has been studied by many golf researchers over a period of more than 30 years in order to search for the "truth" that occurs during the golf swing and attempt to help golfers accomplish the perfect swings according to that "truth".

The first systematic research into the mathematical and biomechanical aspects of golf swing techniques was carried out by the Royal Society Golf Group [2]. In their work, the golf swing was modelled as a planar two-link system named the "double pendulum". The validity of this model has been confirmed by many researchers through actual swing experiments. That is, the known inputs for the model (input torques of shoulder and wrist) would result in the outcome that is very much the same as that from the real golfers' swings. For example, Cochran & Stobbs [2] reported that elite golfers showed marked similarities to the "double pendulum" and that this model was an excellent mathematical analogue of the golf swing. Jorgensen [1] used the assumed constant shoulder torque to drive the model, and the club head speed was found to be consistent with that from a professional's swing. Some researchers such as Campbell & Reid [8] and Sprigings & Neal [10] proposed a three-segment planar model in which the role of the torso rotation

was considered, although the validity of this model has not been confirmed by the actual golf swings.

We should note that the above studies have neglected the elasticity of the golf club shaft. Some researchers considered that the vibration of the club shaft during the golf swing was closely related to the golfer's motion, and the displacement of shaft vibration at impact greatly affected the trajectory of a golf ball [6, 24]. The shaft thus should be matched to the golfer's swing speed and hand action [25]. On the contrary, some researchers such as Milne & Davis [7] and Brylawski [26] believed that the shaft flexibility was not dynamically significant during the golf swing.

It has been noted that the club head speed is a function of the sequential segment velocities of the chain link that makes up the golf swing [10]. The wrist joint would thus be expected to play an important role in the golf swing. Over the years, golf researchers have debated what kind of wrist torque can increase the final clubhead speed. In most of their studies, the golf ball was kept constant and the way the wrist action alters the clubhead speed at impact was not given explicitly. In our study, two dynamic models of golf downswing have been established to examine the combined role of the wrist action and the ball position in the improvement of the final horizontal club head speed. One model is the "double pendulum"; and the other is a new model in consideration of the bending flexibility and centrifugal stiffening of the golf shaft, which has been verified by the actual swing experiments. The results from both models clearly show that the positive wrist torque applied at the latter stage of the golf downswing would provide an advantage in the club head speed at impact. From an energy based analysis, it is also found that the application of the positive wrist torque would increase two factors that facilitate the club

head speed: (1) the work produced by a golfer; and (2) the energy transference ratio, and thus the increased club head speed at impact is achieved.

It is noted that a large amount of research has been devoted to improve golfers' swing skills and golf club performance for decades. Among these studies, golf swing robots have formed a large body of literature [6, 12, 27-32]. In these works, professional golfers' swing motions were expected to be emulated by robots and the evaluation of golf club performance to be replaced by robots instead of golfers.

Most of the golf swing robots on the market have two or three joints with completely interrelated motion. This correlation only allows the users of these robots to specify the initial posture and swing velocity. The subtle adjustments during swing motion due to the various features of individual golf clubs and golfers' arms are not possible. The significance of the dynamic interactions between a golfer's arm and a golf club thus has been noted by some researchers [6, 12, 33]. The influence of the dynamic interference force due to the different golf club characteristics on the swing motion has been investigated [6, 12]. However, the effect of humans' arm masses upon the swing motion has not been studied. Therefore, we used a two-dimensional double pendulum model of the golf swing with the normalized parameters to investigate this problem, and found that the arm mass of humans is an important parameter to affect the swing performance.

Considering the vital of the dynamic interactions between a golfer's arm and a golf club, an impedance control method based on velocity instruction is proposed for a golf swing robot to emulate different-arm-mass golfers. A model of a golfer's swing considering the bending flexibility and centrifugal stiffening of the golf shaft is given by

using the Euler-Lagrange principle and assumed modes method. A prototype of golf swing robot with one actuated joint and one passive joint is developed using the impedance control method. The comparison of swing motion is carried out between golfers and the golf swing robot. The results demonstrate that our golf swing robot can simulate the swing motions of different-arm-mass golfers.

References

[1] Jorgensen. T., 1994. The physics of golf, AIP Press, Spring-Verlag.

[2] Cochran. A. and Stobbs. J., 1999. Search for the perfect swing, Triumph Books, Chicago.

[3] Jorgensen. T., 1970. On the dynamics of the swing of a golf club. America Journal of Physics, **38**, 644-651.

[4] Budney. D.R. and Bellow. D. G., 1979. Kinetic analysis of a golf swing. Research Quarterly for Exercise and Sport, **50**, 171-179.

[5] Williams. D., 1967. The dynamics of the golf swing. Quarterly Journal of Mechanics and Applied Mathematics, **20**, 247-264.

[6] Suzuki. S & Inooka. H., 1999. A new golf-swing robot model emulating golfer's skill. Sports Engineering, **2**, 13-22.

[7] Milne. R.D. and Davis. J.P., 1992. The role of the shaft in the golf swing. Journal of Biomechanics, **25**, 975-983.

[8] Campbell. K. R. & Reid. R. E., 1985. The application of optimal control theory to simplified models of complex human motions: The golf swing. Biomechanics, **IX-B**, 527-538.

[9] Sprigings. E. & Mackenzie. S., 2002. Examining the delayed release in the golf swing using computer simulation. Sports Engineering, **5**, 23-32.

[10] Sprigings. E. & Neal. R., 2000. An insight into the importance of wrist torque in driving the golfball: a simulation study. Journal of Applied Biomechanics, **16**, 356-366.

[11] Pickering. W. M. & Vickers. G. T., 1999. On the double pendulum model of the golf swing. Sports Engineering, **2**, 161-172.

[12] Suzuki. S. and Inooka. H., 1998. A new golf-swing robot model utilizing shaft elasticity. Journal of Sound and Vibration, **217**, 17-31.

[13] Ming. A. and Kajitani. M., 2000. Motion planning for a new golf swing robot. Proceedings of 2000 IEEE international conference on system, man & cybernetics (Nashville), 3282-3287.

[14] Lampsa. M.A., 1975. Maximising the distance of the golf drive: an optimal control study. Journal of Dynamic Systems, Measurement and Control, **4**, 362-367.

[15] McLean. J., 1999. Will Sergio's swing hold up? Golf Digest November, 131-135.

[16] Neal. R., Burko. D., Sprigings. E. & Landeo. R., 1999. Segment interactions during the golf swing: 3 segments in 3D. In Herzog & Nigg (Eds.), Proceedings of the 17th Congress of ISB (pp. 690). Calgary: University of Calgary Press.

[17] Hoa. S.V., 1979. Vibration of a rotating beam with tip mass. Journal of Sound and Vibration, **67**, 369-381.

[18] Theodore. R.J., and Ghosal. A., 1995. Comparison of the assumed modes and finite element models for flexible multi-link manipulators. The International Journal of Robotics Research, **14**, 91-111.

[19] De Luca. A., & Siciliano. B., 1991. Closed-form dynamic model of planar multilink lightweight robots. IEEE Transactions on Systems, Man, and Cybernetics, **21**, 826-839

[20] AE. M., Tang. H. P. and Yokoi. T., 1992. Estimation of inertia properties of the body segments in Japanese athletes. Biomechanism, **11**, 23-33.

[21] M. Mizoguchi., T. Hashiba., T. Yoneyama., 2002. Matching of the shaft length of a golf club to an individual's golf swing motion. In: The Engineering of Sport 4(ed. S. Ujihashi and S. J. Haake), 695-700.

[22] Jones. R., 1966. Bobby Jones on golf, Doubleday, New York.

[23] Hogan. N., 1984. Adaptive control of mechanical impedance by coactivation of antagonistmuscles. IEEE Transaction on Automatic Control, **AC-29**, 681-690.

[24] Butler. J.H., Winfield. D.C., 1994. The dynamic performance of the golf shaft during the downswing. Science and Golf II: Proceeding of the World Scientific Congress of Golf (ed. A.J. Cochran and M. R. Farrally), 259-264.

[25] Iwatsubo. T., Konishi. N. and Yamaguchi. T., 1990. Research on optimum design of a golf club. Transactions of the Japan Society of Mechanical Engineers. **C 56**, 2386-2391.

[26] Brylawski. A.M., 1994. An investigation of three dimensional deformation of a golf club during downswing. Science and Golf II: Proceeding of the World Scientific Congress of Golf (ed. A.J. Cochran and M. R. Farrally), 265-270.

[27] Chen. C.C., Inoue. Y., Shibata. K., 2006. A golf swing robot emulating golfers considering dynamic interactions between arms and clubs.The Engineering of Sport 6 (Volume 3), E. F. Moritz and S. Haake, Eds., Munich, 359-364.

[28] Chen. C.C., Inoue. Y., Shibata. K., Tanioka. H, 2006. Study on the impedance control of a golf swing robot considering dynamic interactions between arms and clubs. The Third Asia Conference on Multibody Dynamics , Tokyo, BM-2, 697

[29] Ming A. and Kajitani. M., 2003. A new golf swing robot to simulate human skill-accuracy improvement of swing motion by learning control. Mechatronics, **13**, 809-823.

[30] Hoshino. Y., Kobayashi. Y. and Yamada. G., 2005. Vibration control using a state observer that considers disturbance of a golf swing robot. JSME international Journal, Series C, **48**, 60-69.

[31] Ming. A. and Kajitani. M., 1996. Human skill and ultra high speed manipulator. Proceedings of 3rd France-Japan Congress and 1st Europe-Asia congress on Mechatronics, 436-441.

[32] Ming. A. and Kajitani. M., 1997. Development of golf swing robot. Proceedings of 3rd Asian Conference on Robotics and Its Application, 41-46.

[33] Chen. C.C., Inoue. Y., Shibata. K., 2005. Study on the interaction between human arms and golf clubs in the golf downswing. The Impact of Technology on Sport, A. Subic and S. Ujihashi, Eds.,Tokyo, 175-180.

[34] Budney. D.R., Bellow. D.G., 1982. On the swing mechanics of a matched set of golf clubs. Research Quarterly for Exercise and Sport, **53**, 185-192.

[35] Neal. R. J., Wilson. B.D., 1985. 3D kinematics and kinetics of the golf swing. International Journal of Sports and Biomechanics, **1**, 221-232.

[36] Milburn. P.D., 1982. Summation of segmental velocities in the golf swing. Medicine and Science in Sports and Exercise, **14**, 60-64.

[37] Dillman. C.J. & Lange. G.W., 1994. How has biomechanics contributed to the understanding of the golf swing? Science and Golf II: Proceeding of the World Scientific Congress of Golf (ed. A.J. Cochran and M. R. Farrally), 3-13.

[38] Lowe. B., 1994. Centrifugal force and the planar golf swing. Science and Golf II: Proceeding of the World Scientific Congress of Golf (ed. A.J. Cochran and M. R. Farrally), 59-64.

[39] McLaughlin. P.A. & Best. R.J., 1994. Three dimensional kinematic analysis of the golf swing. Science and Golf II: Proceeding of the World Scientific Congress of Golf (ed. A.J. Cochran and M. R. Farrally), 91-96.

Appendix

Terminology in golf

1. Golf: a game played on a large outdoor course with a series of 9 or 18 holes spaced far apart, the object being to propel a small, hard ball with the use of various clubs into each hole with a few strokes as possible.

2. Golf swing: the act of swinging a golf club at a golf ball and (usually) hitting it.

3. Swing plane: the imaginary plane in which the player swings the clubhead.

2. Impact time: the instant when the clubhead hits the golf ball.

3. Golf club: the golf club consists of three parts: the clubhead, the shaft and the grip.

4. Clubhead: a fairly narrow metal blade (iron) or a more extended, bulbous shape with a flattish front face (wood) made traditionally of wood but now also made in metal.

5. Shaft: a steel tube or a solid composite tapering down from the grip end to the tip.

6. Grip: a rubber tube which is glued to the butt of the shaft.

7. Clubface: the surface on the head of a golf club used to strike the ball directly.

8. **Natural release point:** the point at which the wrist joint turns freely because of the centrifugal torque of the golf club, even though the input torque about the wrist joint is zero at that moment.

Acknowledgment

I am greatly indebted to my supervisor, Prof. Dr. Yoshio Inoue, for his patient guidance while I was involved in my Ph.D. research work in Kochi University of Technology, Japan. All my research was directed and all my publications including this thesis were corrected by him.

I would like to thank Assistant Prof. Dr. Kyoko Shibata. As my vice-supervisor, she gave me so much help in my research, in particular in the 3th chapter of my thesis the golfer's arm parameters were calculated by the reference that she suggested.

I also would give thanks to my tutor Mr. Akihiro Kimura and Mr. Takashi Mori for their warm-hearted help when I came to Japan. These 'tiny' but kind help such as Japanese character teaching, the Lab introduction and administrative matters of school would be unforgettable.

Thanks would be given to Mr. Yamato Nakano, Mr. Jun Matsushita and Mr. Hajime Tanioka who gave me a lot of help with my experiment. Thanks are also given to Dr. Masafumi Nakahama, whose suggestions on mechanical part choice were very helpful.

I wish to express my gratitude to all the other members of Robotics and Dynamic Lab, who created a very relaxed and comfortable environment for me to conduct my research. Special thanks are given to Dr. Tao Liu and Mr. Rencheng Zheng, who not only gave me much help in my research, but also brought so much laughter and happiness in my daily life.

I also would thank to Special Scholarship Program from Kochi University of Technology and Gakushu Shorei-hi Scholarship from JASSO for their financial support to help me complete my Ph.D. degree.

My most special thanks and gratitude would be given to my lovely wife, Yunjing Meng, whose patience, care and support help me complete this thesis.